
GAZİ ÜNİVERSİTESİ
Gazi
1926

A COMPARATIVE PERFORMANCE ANALYSIS OF GPS POSITION ESTIMATION METHODS

Nurullah GÜRCAN

IN PARTIAL FULFILLMENT OF THE REQUIREMENTS
FOR THE DEGREE OF MASTER OF SCIENCE
IN ELECTRICAL - ELECTRONIC ENGINEERING DEPARTMENT

GAZİ UNIVERSITY
GRADUATE SCHOOL OF NATURAL AND APPLIED SCIENCES

JANUARY 2024

ETHICAL STATEMENT

I at this moment declare that in this thesis study, I prepared the thesis writing rules of Gazi University Graduate School of Natural and Applied Sciences;

- All data, information, and documents presented in this thesis have been obtained within the scope of academic rules and ethical conduct,
- All information, documents, assessments, and results have been presented by scientific ethical conduct and moral rules,
- All material used in this thesis that is not original to this work has been exhaustively cited and referenced,
- No change has been made in the data used,
- The work presented in this thesis is original,

or else, I admit all loss of rights to be incurred against me.

Nurullah GÜRCAN

04/01/2024

A COMPARATIVE PERFORMANCE ANALYSIS OF GPS POSITION ESTIMATION METHODS

(M.Sc. Thesis)

Nurullah GÜRCAN

GAZİ UNIVERSITY

GRADUATE SCHOOL OF NATURAL AND APPLIED SCIENCES

January 2024

ABSTRACT

There are so many applications that require small tolerance to position error. It is so critical for nearly all military and avionics systems. Enhancing the accuracy of position estimation by even a few centimeters is a significant improvement. Estimation errors occur due to a lot of error sources, like multipath effects, ionosphere, and troposphere effects, Doppler shift, clock sensitivity. Besides these sources, mathematically position calculation process after obtaining satellite positions and measuring pseudoranges also causes an error. GPS systems calculate position via the distance between receiver and satellites. An equation is obtained for each satellite the receiver monitors, and the unknowns can be solved by a set of equations. Different mathematical methods have been developed to solve the set of equations. In this study, the effects of three different position calculation algorithms used in literature are compared by means of position accuracy. Satellite positions are learned from a GPS record of a fixed GPS receiver station whose position is known, and a set of equations is formed for receiver position including satellite positions and the distances between the receiver and the satellites. This set of equation is processed with three different position calculation algorithms which are the least squares method, the weighted least squares method and the multilateration algebraic method and calculated receiver position is compared with known receiver position. In the thesis study, model parameters in exponential and sigma model for weighted least squares method are examined. It has been revealed that the weighted least squares method using the exponential model yields the lowest average position estimation error of 7.97 meters. This value indicates a 31% improvement compared to the least squares method.

Science Code	:	90516, 93106
Key Words:	:	GPS, error, least squares, weighted least squares, multilateration, Bancroft, position estimation
Page Number	:	60
Supervisor	:	Prof. Dr. Özgür ERTUĞ

GPS KONUM TAHMİN METOTLARININ KARŞILAŞTIRMALI PERFORMANS ANALİZİ

(Yüksek Lisans Tezi)

Nurullah GÜRCAN

GAZİ ÜNİVERSİTESİ

FEN BİLİMLERİ ENSTİTÜSÜ

Ocak 2024

ÖZET

Çok az miktarda konum hatası toleransına ihtiyaç duyulan birçok uygulama bulunmaktadır. Neredeyse tüm askeri ve havacılık sistemleri için bu durum üzerinde durulması gereken çok önemli bir konudur. Bu yüzden konum tahmininin doğruluğunu birkaç santimetre bile artırmak önemsiz bir gelişme değildir. Konum tahmini hataları, çokyolluluk (multipath) etkisi, iyonosfer ve troposfer etkileri, Doppler kayması, saat hassasiyeti gibi birçok hata kaynağından dolayı meydana gelir. Bu kaynakların yanı sıra, uydu pozisyonları elde edildikten ve ham uzaklık (pseudorange) ölçümleri yapıldıktan sonra uygulanan matematiksel konum hesaplama süreci de bir hata oluşturur. GPS sistemleri, alıcı ile uydu arasındaki mesafe üzerinden konum hesabı yapmaktadır. Alıcı izlediği her uydu için bir denklem elde eder ve denklemin bilinmeyenleri bir denklem kümesiyle çözülebilir. Bu denklem kümesini çözmek için farklı matematiksel yöntemler geliştirilmiştir. Bu çalışmada, literatürde kullanılan üç farklı konum hesaplama algoritmasının konum doğruluğu açısından etkileri karşılaştırılmaktadır. Uydu pozisyonları, konumu bilinen bir sabit GPS alıcı istasyonundan alınan GPS kaydından elde edilmiştir ve alıcı konumu için uydu koordinatları ve alıcı ile uydular arasındaki mesafeleri içeren bir denklem kümesi oluşturulmuştur. Bu denklem kümesi, en küçük kareler yöntemi, ağırlıklı en küçük kareler yöntemi ve çoklaterasyonlu cebirsel yöntem olmak üzere üç farklı konum hesaplama algoritması ile işlenmiştir ve hesaplanan alıcı konumu bilinen alıcı konumu ile karşılaştırılmıştır. Bu tez çaışmasında, ağırlıklandırılmış en küçük kareler yöntemi için üssel ve sigma modellerindeki model parametreleri incelenmiştir. Üstel model kullanılan ağırlıklandırılmış en küçük kareler yönteminin 7,97 metre ile en az ortalama konum tahmin hatası verdiği ortaya çıkarılmıştır. Bu değer, en küçük kareler yöntemine göre %31 daha iyi sonuç alındığnı göstermektedir.

Bilim Kodu	:	90516, 93106
Anahtar Kelimeler	:	GPS, hata, en küçük kareler, ağırlıklandırılmış en küçük kareler, çoklu laterasyon, Bancroft, konum tahmini
Sayfa Adedi	:	60
Danışman	:	Prof. Dr. Özgür ERTUĞ

ACKNOWLEDGEMENTS

Firstly, I would like to thank my supervisor, Prof. Dr. Özgür ERTUĞ, for his guidance to my study.

My thesis would not be possible without the help of my collegues, especially Dr. Şevket GÖĞÜSDERE, Dr. Ahmet Esat SÜZER, Ulvi AÇIKÖZ, Osman Serhat SARAN. I would also like to thank the company I formerly worked, ATEL Technology and Defence, for giving me the opportunity to use laboratory and electronic equipments.

Special thanks to my family, whose constant encouragement fueled my perseverance during the completion of this thesis.

CONTENTS

Page

Page

LIST OF TABLES

Table **Page**

LIST OF FIGURES

Figure **Page**

Figure **Page**

LIST OF MAPS

Map **Page**

SYMBOLS AND ABBREVIATIONS

The symbols and abbreviations used in this study are presented below, along with their explanations.

Symbols	Explanations
GHz	Gigahertz
km	Kilometer
km/h	Kilometer per hour
m	Meter
mm	Milimeter

Abbreviations	Explanations
3D	Three Dimensional
AMC	Alternate Master Clock
DGPS	Differential Global Positioning System
DLL	Delay Lock Loop
DOP	Dilution of Precision
ECEF	Earth Centered Earth Fixed
ECI	Earth Centered Inertial
EKF	Extended Kalman Filter
GDOP	Geometric Dilution of Precision
GLONASS	Globalnaya Navigazionnaya Sputnikovaya Sistema
GNSS	Global Navigation Satellite System
GPS	Global Positioning System
HOT	Higher Order Terms
HDOP	Horizontal Dilution of Precision
IAC	Information and Analytical Center
IGS	International GNSS Service
ILS	Iterative Least Squares
LOS	Line of Sight
LS	Least Sqaures

Abbreviations	Explanations
MEDLL	Multipath Estimating Delay Lock Loop
PDOP	Position Dilution of Precision
PLL	Phase Lock Loop
RTCM	Radio Technical Commission for Maritime Services
RINEX	Receiver Independent Exchange Format
SNR	Signal to Noise Ratio
TDOP	Time Dilution of Precision
TEC	Total Electron Count
USA	United States of America
VDOP	Vertical Dilution of Precision
WGS	World Geodetic System
WLS	Weighted Least Squares

1. INTRODUCTION

Making human life easier is one of the fundamental purposes of technology. In the digital era we are in, the development of technology and its integration into our daily lives are happening rapidly. Among the technologies developed in the last century, one of the most important and widely used is the GPS (Global Positioning System). Considering that the GPS system is used in every phone, ship, and plane produced, the number of users can be expressed in billions. Therefore, it can be said that it is one of the most widely used technologies today.

The GPS system aims to calculate the position and velocity of an object worldwide. Additionally, with its atomic clocks, it provides high-precision time information. These features have made the GPS system, originally designed for military purposes, a favorite in many different civilian sectors. Numerous examples of GPS system usage can be given, such as location determination with navigation applications on phones, enabling planes to land safely on rough terrain, and learning how much ground movement earthquakes cause.

The GPS system designed and managed by the United States is not the first global positioning project. The Transit system, which was active between 1958 and 1996, provided global positioning services with a total of 36 satellites. This system operated on the principle of Doppler frequency shift. In more detail, the frequency of the electromagnetic wave broadcasted by a satellite rises as the satellite approaches to receiver and decreases as it goes away. Based on the change in frequency, it was possible to determine how far the satellite was from the ground station. Once the position of the satellite position was known, the position of the receiver on the Earth could also be calculated. To make this calculation, the receivers needed equipment with highly accurate clocks capable of measuring frequency.

Between 1963 and 1966, The Aerospace Corporation developed a new system that did not require expensive receivers for measurements to be made by four satellites. Unlike the expensive space segment and control stations on Earth of the GPS system, the receiver segment required extremely cheap equipment, which is one of the main differences that distinguishes GPS from the previously used global positioning system called Transit. Thanks

to this concept, even small receivers that can fit into phones can benefit from global positioning services [1].

The GPS system, whose first satellite was launched in 1978, became fully operational in 1994. After the incident in 1983 when a Korean Airlines plane deviated from its route and was shot down after entering Soviet airspace, it was decided to open the GPS system to civilian use with selective availability restrictions. The selective availability implementation was removed in 2000, allowing civilian applications to receive services more accurately. Today, the GPS system continues to provide global positioning services with 31 satellites in orbit.

The GPS system aims to transmit the data necessary for calculating the coordinates of a receiver at any point on Earth through satellites. To calculate its own coordinates, the receiver needs to know the distance to observed satellites and the positions of these observed satellites. If the receiver just knows the position of one satellite and the measured range to that satellite, its possible position is on a sphere surface whose center is at the satellite's location with a radius equivalent to the distance to the satellite. Figure 1.1. shows an example for a receiver knows its distance from only the satellite “A” which is 25 000 km.

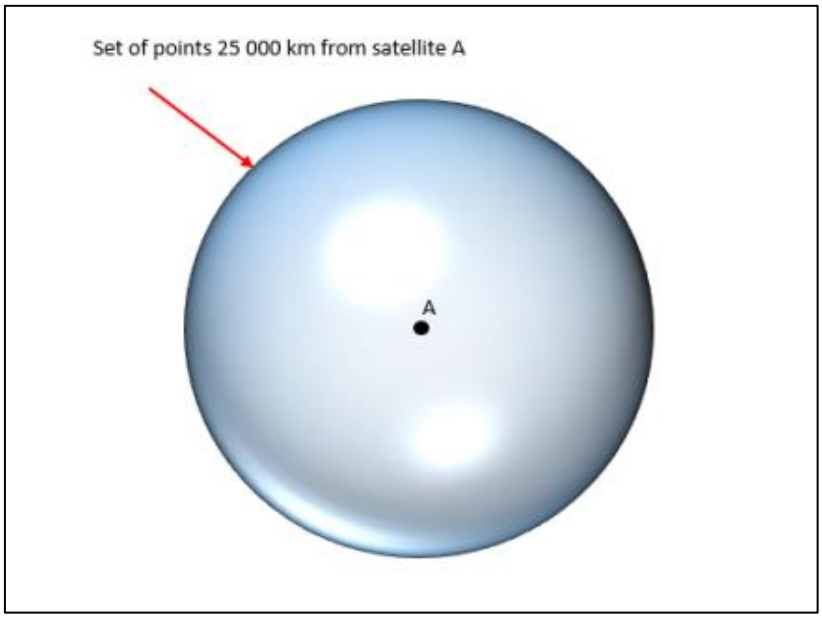

Figure 1.1. Possible receiver locations in case only one satellite is observable [2]

If the receiver knows the positions of two satellites and the distances to them, its possible location is on the intersection circle of two spheres whose centers are at the respective satellites. As seen in Figure 1.2., a receiver observes two satellites. If it is assumed that the receiver measured the distance to satellite “A” as 25 000 km and the distance to satellite “B” as 35 000 km, possible receiver location is limited by the interception of two spheres. The two spheres must intercept somewhere if the distances calculated correctly.

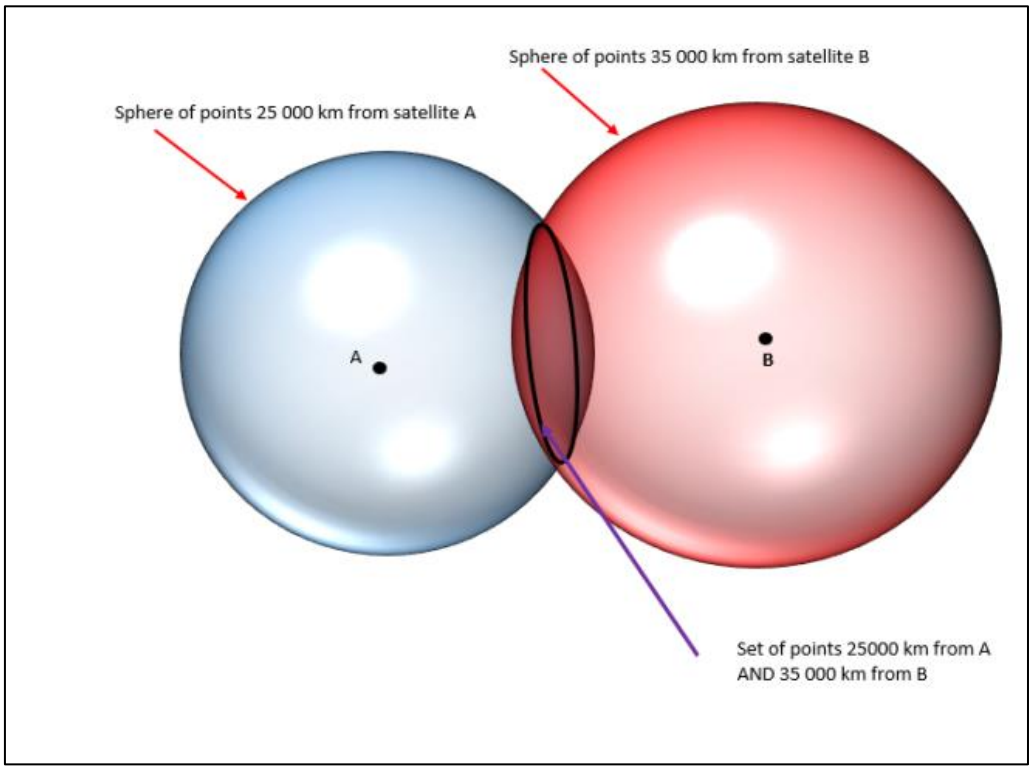

Figure 1.2. Possible receiver locations in case only two satellites are observable [2]

For three satellites, the possible location of the receiver is only at two points which are the intersection points of three spheres whose centers are at the satellites’ positions. In Figure 1.3., it is shown that the receiver observes three satellites. The distance between the third satellite “C” and the receiver is assumed as 21 000 km and the interception points of three spheres are indicated by purple arrows. One of these points is too far from Earh and the other one refers the receiver positon on Earth surface. This method using the interceptipon of three spheres is called trilateration.

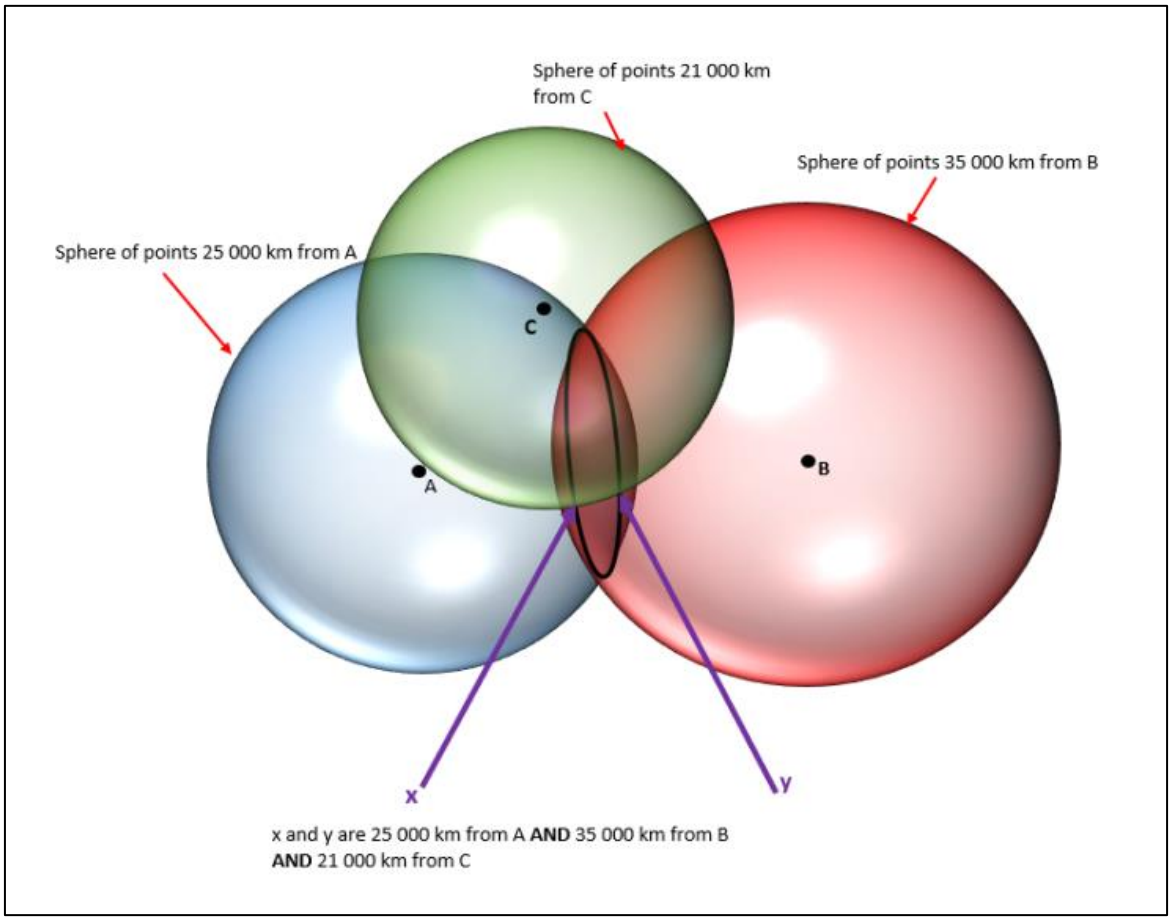

Figure 1.3. Possible receiver locations in case three satellites are observable [2]

Based on this explanation, one might think that the receiver needs data from three GPS satellites to calculate its position. From a different perspective, the receiver needs to know its coordinates on the X, Y, and Z axes to calculate its position on Earth. Assuming each coordinate on these axes is unknown, the receiver would need data from three satellites to solve three unknowns. However, precise measurement of the signal's time in the air is essential to calculate the distance between satellites and receivers. Although atomic clocks in GPS satellites allow accurate time measurements, receivers generally have inexpensive and low-precision clocks. This situation arises one more unknown for the receiver as what the timing error of the receiver is in comparison to GPS master clock. To figure out the time difference between the receiver's clock and the GPS satellite's clock, data from an additional satellite would be required. Therefore, in the worst-case scenario, the receiver must have the data from at least four GPS satellites to estimate its position. Since some of marine applications do not need to know its height over the sea level, three GPS satellites would be enough for them to calculate the uncertain parameters for the receiver as X, Y coordinates and the timing error.

GPS error budget

There are so many applications that require small tolerance to position error. It is so critical for nearly all military and avionics systems. Enhancing position estimation accuracy a few centimeters is not insignificant improvement. Therefore, many studies have been conducted on estimating and eliminating of error sources in the literature. Because GPS system dates to sixties, a lot of problem is solved using different techniques. Nevertheless, people still study on GPS system to find more practical and easier ways to problems.

Estimation errors occur due to a lot of error sources, like multipath effects, ionosphere, and troposphere effects, Doppler shift, clock sensitivity [3]. Besides these sources, mathematically position calculation process after obtaining satellite positions and measuring pseudoranges also causes an error. In addition to satellite coordinates and distance data, the GPS system provides various error correction data to ensure the accuracy of the received information. These error correction data are crucial for precise calculation of the receiver's position. In the past, an intentional error was added to the distance between satellites and receivers to decrease the position accuracy for civilian use. However, this practice was discontinued in 2000 due to the broader applications of GPS in sectors like marine and aviation, where accuracy is crucial for human safety.

Ionosphere and troposphere

Briefly mentioning the error correction data in the GPS system, it is essential to note that signals from GPS satellites, approximately 20 000 km above the Earth's surface, pass through atmospheric layers with varying gas densities. The slowdown caused by the troposphere and ionosphere layers with different gas densities leads to an overestimation of receiver’s the measured range to the satellites. To correct this, signals are sent at different frequencies, and the timing bias between their arriving moment is employed to calculate error correction data.

The ionosphere can have a significant impact on GPS signals. The ionosphere is a layer of the Earth's atmosphere which involves charged particles. Although different approaches exist on the limits of the ionosphere, it can be said that it is located approximately 30 to 600 kilometers above the surface of the Earth. This layer can cause several influences on GPS

signals, including signal delay, dispersion, bending, and scintillation. Due to the existance of free electrons, the speed of light in the ionosphere is slower than in a vacuum, resulting in frequency-dependent signal delays. Ionospheric dispersion causes different frequencies to experience varying delays, leading to signal spreading and potential inaccuracies in position calculations. Additionally, the ionosphere can bend GPS signals, introducing errors in estimating user positions. Under specific conditions, scintillation occurs, causing rapid fluctuations in signal amplitude and phase, particularly in equatorial and high-latitude regions. These ionospheric effects necessitate correction techniques in GPS systems to enhance positioning accuracy. To mitigate the impact of the ionosphere on GPS, various correction techniques are employed. Differential GPS (DGPS) is one such technique that uses an additional reference station to scale ionospheric errors. Additionally, the GPS system itself incorporates models and algorithms to estimate and compensate for ionospheric effects, providing more accurate positioning information to users.

Ultraviolet rays spreading from Sun ionize some gas molecules, resulting to arise free electrons [4]. These charged particles can cause several influences on GPS signals, including signal delay, dispersion, bending, and scintillation. Figure 1.4. shows added transmission delay in GPS signals in ionosphere and troposhere due to high total electron content (TEC) involving particles which distorts electromagnetic wave [5].

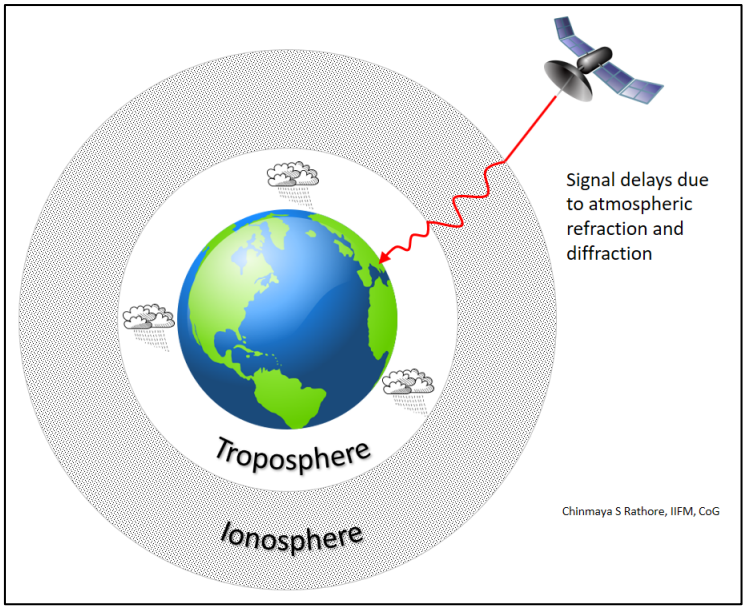

Figure 1.4. Ionosphere effect on GPS signal [5]

L. Zhao, Li, and X. Zhao published a paper in 2009 which recommended a novel method for designing the adaptive Hatch filter with optimal weigting factors. Their method depended on on examining the positioning error due to ionosphere temporal and spatial gradients and multipath effects. While traditional Hatch filter improves positioning accuracy in exchange for diverging filtered errors, experimental results of recommended model showed that novel model provides more accuracy in terms of positioning results than the traditional Hatch filter [6].

In the paper published by Sucharoen, Wu, and Weng in 2015 focused on plasma blown from solar stroms which causes particle disturbance in the ionosphere. Unstable nature of ionosphere layer makes the particles irregular. So, it is hard to put a model independent from time and location for ionosphere to mitigate related error. This paper examined the properties of ionosphere in equatorial and middle latitude zones during solar maximum by analyzing GPS data in Thailand and Australia. The research showed that characteristic of total electron content variation is influenced by the solar activity. Additionally, another finding indicated that the electron density in the equatorial ionosphere zone is higher compared to the middle latitude ionosphere zone. Consequently, this suggested that the error in GPS measurements caused by the ionosphere over the equatorial ionosphere zone would be greater than the observed ionospheric error over the middle latitude zone [7].

Akiyama, Tanaka, and Yonekawa proposed a new method to improve positioning accuracy by ionospheric delays in the paper published in 2007. Their method was based on using approximation of double frequrncy correction. It was mentioned that new double frequency method effectively enhances precision beyond that achieved by traditional correction methods in both horizontal and vertical directions simultaneously [8].

The troposphere is lowest atmospheric layer of the Earth. It does not exhibit dispersion for the frequencies up to 15 GHz. It introduces several effects on GPS signals. Firstly, water vapor in the troposphere causes delays in GPS signals, and unlike the ionosphere, these delays are generally consistent across the various GPS frequency bands. Additionally, the variation in air density within the troposphere leads to atmospheric refraction, causing GPS signals to bend as they pass through. This atmospheric bending can impact the accuracy of position estimates, particularly when signals traverse different atmospheric conditions. Although the troposphere primarily affects signal delay, there can also be some degree of

signal dispersion due to its water vapor content, although this effect is typically less pronounced than in the ionosphere. Advanced correction models and techniques, such as Differential GPS, are applied to mitigate these tropospheric impacts and enhance the precision of GPS positioning.

Phase and codes are equally delayed in troposphere layer regarding free space propagation. While these delays reveal itself as 2.4 meters for a satellite located on a perpendicular projection to Earth's surface, the error goes up to 25 meters for a receiver at see level if the satellite is observed at an elevation angle of 5° [4]. This effect especially leads to incorrectly calculate the height of receiver.

Guo, Yang, Shi, and Xu published a paper in 2016 which proposed an optimal weighting method for functional model of GPS troposphere tomography equations. These equations consist of the observation equation, the horizontal constraint equation, and the vertical constraint equation. In contrast to conventional equal and constant weighting schemes, the proposed method allows adaptive adjustments of weights. Numeric outcomes, acquired under diverse weather conditions, illustrated that the suggested approach substantially improves the precision of GPS tomography modeling, particularly when compared to the traditional constant weighting methods [9].

In the paper published in 2007, Wang, Liou, and Yeh investigated the tropospheric influence on estimation of height which is primarily caused by water vapor inhomogeneity. They used the data collected in 2003 from 21 GPS receivers which were built as fixed reference stations. The meteorological measurements which consist of temperature, pressure, and humidity defined to GPS data processing algorithm with 24 troposheric parameters. Calculated receiver heights without and with a priori knowledge of meteorological measurement are examined. These measurements had a notable importance on calculated height. Daily correction can be potentially reaching to 9.3 mm for the identified cases [10].

In the paper published in 2019, Koohzadi, Ebadollahi, Vahidnia, and Dian examined various traditional tropospheric delay models and combinations of multiple models to ascertain real-time positions. These models were integrated into the real-time positioning algorithm for a single-frequency GPS receiver and were subsequently compared. Real-time positioning experiments were conducted in six iterations over the course of six days. The comparative

analysis revealed that the Modified Saastamoinen model has better accuracy for real-time positioning of single frequency GPS receiver. The accuracy of the Modified Hopfield model is sufficient for low-cost real-time positioning due to its shorter computation time [11].

Multipath

The signals broadcasted by GPS satellites travel in waves towards the Earth's surface, where the receiver's antennas capture both the electromagnetic waves reflected from the Earth's surface and the directly transmitted waves. Multipath errors, arising from waves reaching the receiver through different paths, can significantly impact position accuracy, especially in urban environments. The signal sent by satellite propogates and grows as waves in space. Each satellite is above 20 000 km above Earth surface so that signal transmitted by satellites is able to serve very large area on Earth surface. The point which gets strongest signal is the projection point of satellite on Earth surface. Thus, a receiver which sees a satellite over the top of its location gets most powerful possible signal from that satellite. However, the signal In order to transmit the signal from the satellite to the reciver most effectively, a line of sight (LOS) must be established through the receiver and the satellite. In addition to that, the antennas of both the satellite and the receiver must be aligned towards the directions where their gains are strongest. These conditions hold true under normal conditions with no environmental interference between the satellite and the receiver. When it comes to a real case scenario, the receiver not only captures the signal which follows line of sight pattern, but also gets the same signal which reflects from objects and terrain in its vicinity. Figure 1.5. depicts this scenario.

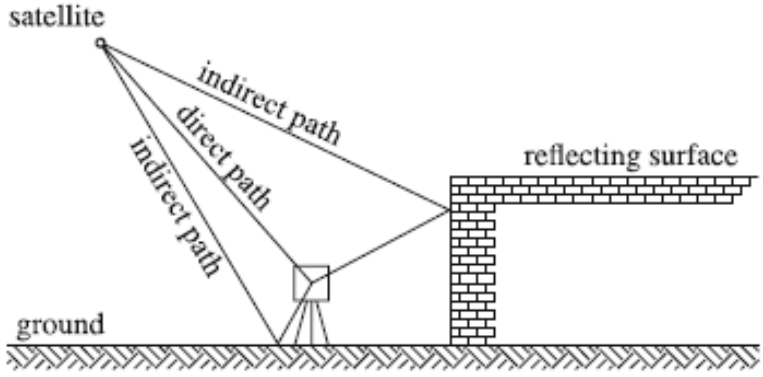

Figure 1.5. Visualization of multipath effect [12]

Each signal which follows different paths reachs the receiver antenna with changes in propagation direction, amplitude, polarity, and phase. Thus, two distinct components, direct and indirect, are formed in the signal reached to the receiver. In fact, the indirect component is derived from direct component by adding delays, phase-shifts, and attenuates. Due to the delay and phase shift, the two signals can interfere with each other. When they are in the same phase, their total amplitudes can sum up. When they are in opposite phases which is more often case, they can create a 180-degree phase difference. So, they can cancel each other out.

A real illustration of code and phase delay due to the multipath effect is shown in Figure 1.6. While code and phase delays must be formed at a certain time in an ideal condition, different time delays are seen for a multipath effected environment. In Figure 1.6., first illustration shows constructive multipath interference, and second illustration shows destructive multipath interference. The original triangular correlation function is denoted by the solid thin line, the multipath correlation function by the dashed line, and the sum of the two by the third line [3].

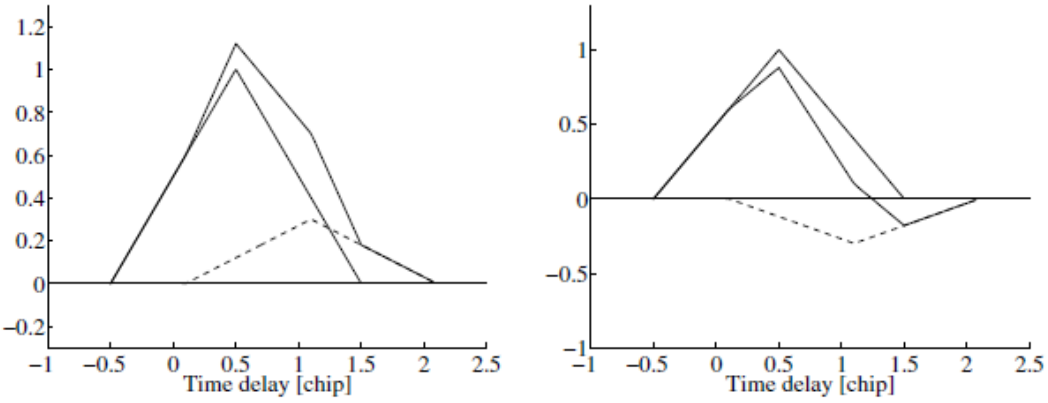

Figure 1.6. Constructive and destructive multipath effects [3]

A mathematical model demonstrating the multipath effect does not exist because it is a problem dependent on both time and location. Nevertheless, the error in the receiver's position calculation due to this effect can be observed through phase measurements of two different frequencies broadcast by GPS satellites. The fundamental principle here is that two signals at different frequencies cover the same paths and are exposed to the same environmental effects until they reach the receiver. Since they both originate from a single antenna on the satellite and reach the sane antenna in the receiver. The tropospheric error,

time error, and relativistic effects are equal for two signals at different frequencies. However, since the ionospheric and multipath effects are frequency-dependent, these errors are not same for signals at different frequencies. When the ionospheric effect is eliminated using different solution methods, only the multipath effect can be observed between signals of different frequencies. Residual error, excluding the noise level, are thus considered as multipath error [12].

In the past, numerous studies have been conducted in the areas of measuring and mitigating the multipath effect. In a paper published in 2000, Minami, Morikawa, and Aoyama discussed the multipath effect as one of the fundamental error sources in GPS. They detailed a technique to predict the multipath effect in measurements which reduces both code and carrier multipath errors. This technique involved using an adaptive filtering process to predict parameters of both the directly received signal and the signal coming from the multipath. They explained how the multipath effect manifests itself during the tracking stage of GPS signal processing, causing lock errors in traditional Delay Lock Loop (DLL) and Phase Lock Loop (PLL) hardware when finding code and phase delay. They noted that in the past, methods were proposed only for decreasing multipath errors in DLL, followed by the suggestion of a system called MEDLL (Multipath Estimating Delay Lock Loop) that included both DLL and PLL hardware which requires several correlators as a disadvanteage. In their proposed adaptive filtering method, they used a multipath delay profile to facilitate a simple multipath estimation. Simulation results demonstrated that their method produced a reliable solution with high accuracy in a multipath environment [13].

In 2011, Phan and Tan published a conference paper which utilizes a nonlinear regression model to mitigate the multipath effect. They placed a GPS receiver on the top of a building and trained the model based on the assumption that each satellite follows a repetitive orbit geometry relative to their fixed receiver on the Earth's surface. Subsequently, they applied this model to diagnose and mitigate multipath errors in a receiver environment with the presence of the multipath effect. They observed an increase in position accuracy of 25-35% in measurements with the influence of multipath [14].

In the conference paper published in 2021, Kim, Lee, and Park approached the problem from a different perspective, performing multipath error detection based on the carrier-to-noise density ratio which is obtained via dual polarized antennas. While the right-handed antenna

was sensitive to satellite signals, the left-handed antenna was sensitive to reflected signals. So, the difference between them revealed as the multipath effect. This effect was tested using measurements obtained from real-world scenarios [15].

Relativity

Atomic clocks used in GPS satellites have so large gravitational and motional frequency shifts. While gravitational effect is caused by general relativity, motional effect is caused by general relativity. System would not work if relativistic effects do not take into account. For example, a deviation in timing of one nanosecond will result in positioning inaccuracies on the scale of approximately 30 centimeters. Although satellite velocities are relatively small and gravitational fields are weak in proximity to Earth, they still induce notable relativistic effects. The article published by Neil Ashby in 2003 is a useful source to understand relativity effect in the GPS [16].

GPS satellites orbit the Earth twice a day at an average velocity of 14 040 km/h relative to Earth. Additionally, the Earth spins around itself at an angular velocity of about 1 600 km/h. Considering the magnitude of these velocities, relative motion of satellite compared to a receiver is noticeable. Theory of special relativity says that time is relative, and it can be dilated depending on the relative velocity between two observers. Since a receiver on Earth sees the GPS satellites in motion relative to itself, the receiver on Earth sees clock of GPS satellites operating more slowly as per special relativity. This means that on-board atomic clocks on the satelites falls behind clocks on the Earth by approximately 7 microseconds per day. This discrepancy arises from the slower ticking rate caused by the time dilation effect resulting from their relative motion [17]. If this effect is ignored, the timing error would be increased cumulatively and position accuracy on the order of centimeters would not be achieved.

The orbits of GPS satellites are high above the Earth. The curvature of spacetime caused by the Earth’s mass is less powerful at the orbits of satellites compared to the Earth’s surface. According to general relativity theory of Einstein, a clock under an influence of gravity seems to run slower than a clock at a distant region which is subjected to less gravitational force. Therefore, clocks on Earth tick slower compared to clocks on GPS satellites in orbit [18]. Applying the principles of general relativity, the clocks in each GPS satellite are

expected to advance ahead of ground-based clocks by approximately 45 microseconds per day [19]. This relativistic effect must be considered for the need for high accuracy in military applications.

To ensure the accuracy of GPS, corrections are made for both of these relativistic effects. The satellite clocks are updated to account for the time dilation due to their relative high speed and their altitude in the Earth's gravitational field. The corrections are built into the satellite clocks and are regularly updated to maintain the precision required for GPS navigation.

Ruyong Wang published a paper in 2000 which re-axamine special relativity and Sagnac effect using pseudrange equation. In this paper, it is emphasized that the computations utilizing the pseudorange equation indicate that the accuracy of the equation contradicts the two principles of special relativity, the principle of the constancy of the speed of light and the principle of relativity. Additionally, the Sagnac effect can be entirely explained by this equation, suggesting that the Sagnac effect is a non-relativistic phenomenon. It has been suggested that the relativity of simultaneity in special relativity conflicts with the fundamental operational principle of GPS [20].

Clock synchronization

Clock synchronization has a vital importance on GPS concept. A receiver on Earth calculates its position based on satellite coordinates and the distances between satellites and itself. It is so essential that all this information must be valid exactly for the same moment from the viewpoint of the receiver. Thus, the receiver can decide its location using trilateration method.

Each GPS satellite transmits the ephemeris information in a two-hour period which includes satellite coordinates at a certain epoch. In addition to that, the satellites transmit navigation message that includes transmit time, allowing the receiver to calculate travel duration of signal. Timing is important as seen in both of two steps. If one of the satellite clocks runs slower than others, the satellite would record its coordinate on its orbit with a delay and broadcast the transmit time of navigation message incorrectly. Since the receiver uses the distances between multiple satellites and itself which is determined by the traveling time of

the signal and satellite coordinates at a certain epoch, any incorrect measurement about a couple of nanoseconds would cause a misestimation of receiver positon on the order of meters. Therefore, all clocks of satellites must share common time and must be synchronized to master station periodically.

GPS satellite clocks are synchronized through a coordinated process involving ground control stations and onboard atomic clocks. Ground control stations, integral parts of the GPS control segment, continuously monitor the performance of atomic clocks on each satellite, collecting data on any deviations from the expected time. Using this data, the ground control stations calculate precise clock corrections, addressing factors such as clock aging, environmental conditions, and relativistic effects. These corrections are then uploaded to the respective satellites during communication sessions. Then the satellites add this information to the navigation message when broadcasting the signal. Onboard, each GPS satellite is equipped with highly stable atomic clocks, typically Cesium or Rubidium clocks, serving as reference time for the satellite and timing signals transmitted to GPS receivers on Earth. The synchronization process also includes adjustments for relativistic effects, ensuring that the satellite clocks remain accurate despite their high-speed orbital motion and position in the Earth's gravitational field. This meticulous synchronization is crucial for maintaining the overall accuracy of the GPS system, enabling precise determination of signal travel times and accurate positioning for GPS receivers worldwide.

The GPS satellites and control stations uses atomic clocks depends on generally Cesium clock and fewer number of Rubidium clock. The atomic clocks in satellites, synchronized by the master station in the control segment, may still have small time differences due to orbital motion. This slight discrepancy contributes to a margin of error in distance measurements between satellites and receivers. Figure 1.7. shows that Allan deviation for Quartz and Cesium clocks. While Cesium are extremely accurate atomic clocks used in GPS satellites, Quartz can be found in a typical GPS receiver. Quartz oscillators are more stable for a short duration as seen in Figure 1.7. It is clear that Cesium shows better performance after 100 seconds according to the plot. A Cesium clocks are so stable that their accuracy in a day is within 4 nanoseconds if no relativistic effect is existed [16].

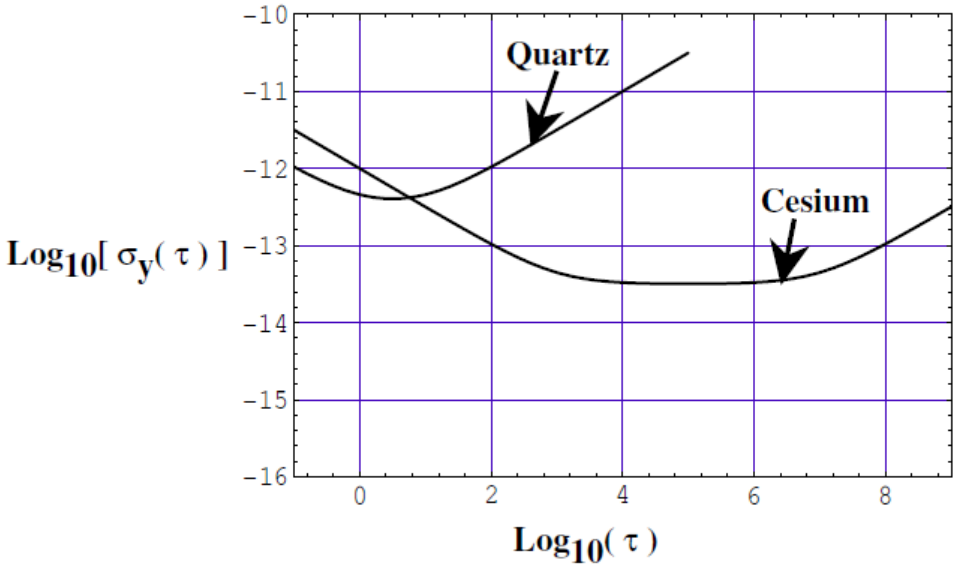

Figure 1.7. The Allan deviation of Cesium clocks and Quartz oscillators over time [16]

In 2013, Cernigliaro, Galleani and Tavella published a paper which made any analysis on space clocks of GNSS. They made a performance analysis for GPS and GLONASS (Globalnaya Navigazionnaya Sputnikovaya Sistema) clocks, by using the satellite clock estimates produced by the Information and Analytical Center (IAC) of the Russian Federal Space Agency. A few preliminary results of this analysis were discussed. The examination focused on assessing the time deviation, frequency deviation, and frequency stability of Cesium and Rubidium clocks installed on three GPS and GLONASS satellites. The findings revealed the existence of two recurring anomalies in space clocks, specifically deterministic oscillations, and frequency jumps [21].

Dilution of precision

The arrangement of visible satellites plays a crucial role in attaining high-quality results, particularly in point positioning and kinematic surveying. Dilution of precision, shortly DOP, is a measure of the instantaneous geometry of GPS satellites. The geometry satellites relative to a receiver on Earth changes with time due to relative motion of the receiver and the satellites [12]. Therefore, it is necessary to determine the orbits and the number of satellites very carefully. Dilution of precision indicates how well the satellites placed for a receiver on Earth. The lower the dilution of precision value, the more accuate estimation of receiver position. While DOP value smaller than 1 is accepted as the top confidence level to

be employed for applications that consistently require the highest attainable sensitivity, DOP value bigger than 20 accepted as the measurements should be discarded.

Figure 1.8. shows the impact of the good and bad examples for dilution of precision. The transmitters represent the GPS satellites. Red curve is plotted based on the calculated distance between the receiver and transmitter 1. Because each measurement has an error due to lots of sources, other pink curves is plotted to show maximum and minimum possible distances in real. Same situation can be considered for the green curves representing the transmitter 2. Thus, the distances from two transmitters intercepts in an area filled with orange which means the receiver must be somewhere in interception area. The transmitters in other words satellites are close to each other in the second illustration compared to the first one. As seen in Figure 1.8, the interception area in the second illustration is bigger which implements that the sensitivity of the position accuracy is worse than the first illustration. It can be figured out that wider separation of satellite geometry on sky yields more accurate estimation of receiver position.

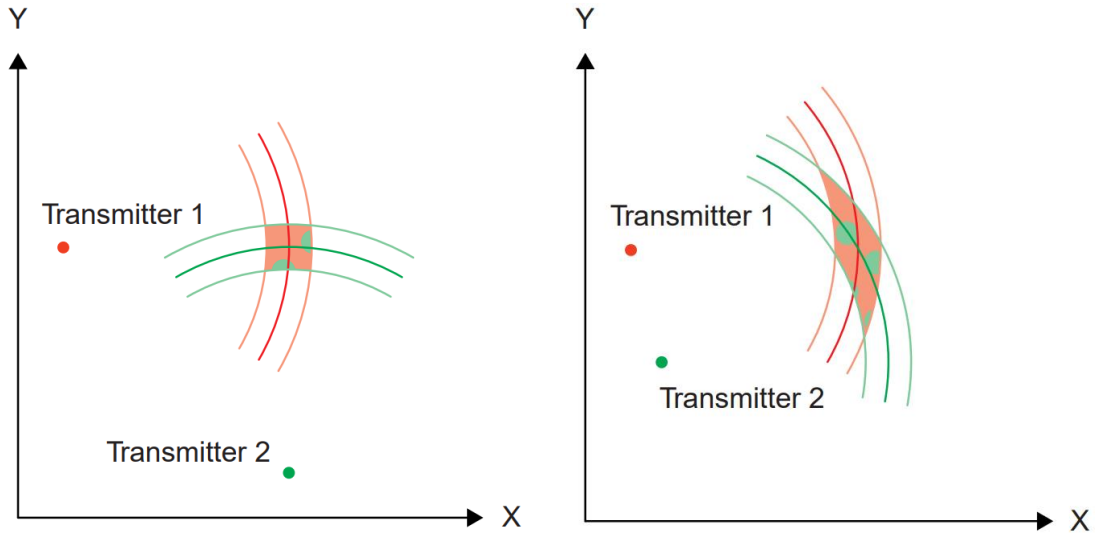

(a) (b)

Figure 1.8. Effect of the satellite constellation on position accuracy [22]

The constellation must provide that a receiver located anywhere on Earth must continuously observe at least four satellites and all satellites must form a geometry that has low dilution of precision. To go into details, a road which has buildings on both sides or a canyon which let a limited vision of sky blocks the signal from satellites for a receiver in a mentioned environment. The observable satellites for a receiver are decreased compared to open sky.

So, the receiver must calculate its position using the satellites visible above it. If GPS satellite constellation is not enough to provide sufficient number of satellites, such a receiver can not estimate its location.

The objectives of DOP can be classified into three stages. Initially, it aids in survey planning, and subsequently, it can assist in interpreting processed baseline vectors. For instance, data exhibiting poor DOP might be considered for exclusion. Ultimately, DOP projects errors from the measurement domain onto errors in the position domain [12]. There are some subheadings related to dilution of precision. GDOP (geometric dilution of precision) indicates geometric accuracy in position and time. PDOP (position dilution of precision) represents accuracy in position. TDOP (time dilution of precison) shows how accurate is the measurement in time. HOP (horizontal dilution of precison) is the accuracy of horizontal positon. VDOP (vertical dilution of precison) is the accuracy in vertical direction.

Tahsin, Sultana, Reza, and Haider published a paper in 2015 which analyzes DOP and its preciseness in GNSS position estimation. They introduced the different kinds of DOP, namely GDOP, PDOP, HDOP, VDOP, TDOP and derived a comparative conclusion on DOP among GPS, Galileo and combined GPS and Galileo satellite configuration. The calculation they made showed that wider the angular separation between satellites, lower the DOP. Compared to the performance of GPS, Galileo demonstrates enhanced precision. Utilizing a receiver that combines both GPS and Galileo can be advantageous in such scenarios [23].

Overdetermined pseudorange equations

The disruptive effects of the Earth's atmosphere, the time difference between GPS satellites, and the signal reaching the receiver through different paths are issues that occur independently from the receiver. The issue of not being expensive and accurate for the receiver's clock is already a problem that the GPS system addresses by using four satellites. Even after solving other problems brought by the system, position errors which derive from the receiver can still arise. After the necessary satellite coordinates and distance information between satellites and the receiver for the receiver's location are obtained, and the effects of the mentioned error sources are eliminated, the receiver can calculate its position

inaccurately. So, faulty mathematical operations can lead to all efforts which performed before being in vain.

Pseudorange is the distance between the receiver and the satellites involving errors. Like forming the equation of a line with two known points, pseudorange equations are constructed similarly with one point being the satellite coordinates and the other point being the receiver coordinates. In pseudorange equations, satellite coordinates are known, while receiver coordinates on each axis and the timing error are unknown.

Once the necessary data from at least four GPS satellites are received, the receiver creates a system of four unknowns using pseudorange equations. The orbits of GPS satellites are designed to ensure visibility of at least six satellites from any point on Earth, providing at least six pseudorange equations under normal conditions. This situation leads to a problem called overdetermined system in mathematical literature. To make the issue clearer, a set equation can be considered involving $y = x + 5$ as a first equation, $y = 2x$ as a second equation, and $y = x + 9$ as a third equation. It is noticeable that there are three equations corresponding to two unknowns as x and y. No exact is exist fot the values of x and y which is valid for all three equations. In the scenario of GPS, there are generally at least six equations corresponds to four unknowns as 3D coordinates and time difference. Similar to previous example, the solution of unknowns in GPS can not be calculated using traditional algebraic methods.

Although overdetermined systems do not have a common solution set, various solution methods that aims to converge to the most accurate result possible has been developed. These methods are based on least squares, weighted least squares (WLS), algebraic method using multilateration, Kalman filter.

In the conference paper published in 2013, Tian, Dong, Ning, and Fu gave an overview of nonlinear least squares methods for estimating receiver position. They presented GPS satellite pseudo-range observation equations by true GPS receiver and linearization of these equations by Taylor expansion model. Weighted least squares method was used in simulation. Although they mentioned weighting was based on elevation angle of observed satellites, no numerical values were presented. The simulation results showed that weighted least squares iterative algorithm is straightforward and rapid [24].

In the paper published by Li and Wu in 2009, they presented a study about determining weight elements based on SNR (signal-to-noise ratio) to be used in weighted least squares method. They proposed a novel weight model employing an exponential function, and the weight factors are normalized to calibrate the positioning accuracy. A thorough analysis of the impact of parameters in the exponential model on positioning accuracy is conducted, leading to the careful determination of these parameters. They tried different coefficients for weights and decided the ones which gives most accurate result resulting least error. In contrast to the positioning solution without weight and the sigma model, there was a noticeable improvement in positioning accuracy, particularly at points with significant bias. The lower the PDOP, the more precise the positioning solution [25].

In the paper published on 2014 by Doma and Sedeek, the estimation of GPS receiver position using iterative least squares and extended Kalman filter was investigated. They focused on determining the receiver coordinates for a fixed point using pseudorange measurements from a single GPS receiver. The estimation of unknowns was accomplished by incorporating both an Extended Kalman Filter (EKF) and Iterative Least Squares (ILS) in the processing. Kalman filter, used often nowadays, elies on specific assumptions, and when these assumptions are satisfied, it can provide optimal estimation and prediction. The Extended Kalman Filter (EKF) not only demonstrated practical effectiveness but also possessed theoretical appeal, as it was proven to be the filter that minimizes the variance of the estimation mean square error. From the result of this study, Extended Kalman Filter was more quality than Iterative Least Squares method [26].

Stephen Bancroft published a paper in 1985 which proposed a novel method to estimate the position of a receiver. This method depended on an algebraic solution which is noniterative in contrast to traditional least squares method known until that time. It is computationally efficient and numerically stable because of the fact that it only involves algebraic operation. The Bancroft method eases the processing and gets rid of iterations. Additionally, it enhances accuracy in scenarios with poor geometric dilution of precision and enables a cold start in deep space applications [27].

This thesis aims to explore the effects of three algortihms used in solution of overdetermined system for GPS receiver position estimation, namely the least squares method, the weighted least squares method, the multilateration method. A fixed GPS station whose position is

known is used as a reference point, then the solution of three methods is compared with the reference point. The accuracy in X, Y, and Z axes of three methods is calculated and best method yields more precise solution is announced. It is assumed that other error sources do not affect the comparison result. All three methods utilize the satellite positions and the distances between the receiver and the saatellites. Even if this information may include errors due to mentioned sources previously, they will appear on the solutions of the methods equally. So, the method which gives the solution closer to reference is considered as the best one rather than examining the real accuracy of the methods. Because it is known that other error sources deflect real positioning accuracy.

2. CONCEPT OF POSITION ESTIMATION IN GPS

The estimation of the receiver's position primarily depends on GPS satellite positions and pseudoranges. Receivers acquire GPS satellite positions from broadcasted navigation message. Satellite positions are stored as Keplerian parameters in navigation message, so the receiver converts these parameters to Cartesian coordinates which takes Earth center as origin point. Pseudoranges, which indicates travel time of signal between each visible GPS satellite and receiver are measured and calculated at receiver side. As a result, pseudorange equations consist of satellite positions and pseudorange measurements as the same number of visible satellites are obtained.

The GPS system aims to determine the three-dimensional location of a receiver on Earth. Each satellite in orbit sends its position along with time information to Earth at a specific moment. Receivers on Earth calculate the time it takes for the signal to reach them by subtracting the time which the signal was sent from the time which the signal was received. The product of the travel time and the speed of light gives the distance between the satellite and the receiver. Using the distances from different satellites, the receiver calculates its own position.

In a coordinate system with three axes (X, Y, and Z), considering the Earth's center as the origin, there are three unknowns to determine the receiver's position accurately. In addition to the unknowns along the X, Y, and Z axes, there is another unknown due to the working principle of the GPS system. While all GPS satellites have a synchronized clock, the clocks in the receivers are not synchronized with the GPS system. The difference in clock synchronization between the satellite and the receiver leads to errors in distance calculation. Therefore, in the GPS system, there are a total of four unknowns: the time difference of the receiver's clock, and the receiver's position along the X, Y, and Z axes.

From a mathematical perspective, to solve for the four unknowns, at least four equations are needed. If a receiver can observe four satellites, four pseudorange equations can be formed to calculate the distance between each satellite and the receiver. Thus, solving these four pseudorange equations allows the determination of the four unknowns and the calculation of the receiver's position. In other words, the receiver needs to observe at least four satellites

to calculate its own position. However, receivers on Earth usually see more than four satellites simultaneously. Therefore, there will be more than four pseudorange equations for the four unknowns on the receiver's side. This study explores the impact of different algorithms used to solve pseudorange equations on position accuracy.

2.1. Receiver and Satellite Coordinates

Various coordinate systems exist for expressing the position of a receiver on Earth. One such system specifies the receiver's position in terms of latitude, longitude, and altitude. Earth-centered Earth-fixed (ECEF) coordinate systems are used for this purpose, where the Earth's center is the origin and there are three axes (X, Y, and Z). Latitude indicates how far north or south the receiver is from the equator, while longitude indicates how far east or west it is from the Prime Meridian. Altitude defines how high the receiver is from the sea level. Thus, the receiver's three-dimensional position on Earth is defined with the help of these three parameters.

While the notions of latitude and longitude can be used to determine the coordinates of any point on Earth, they are not preferred for expressing the coordinates of celestial bodies like GPS satellites due to the Earth's rotational motion. As the Earth rotates, the Prime Meridian will also move. For a stationary celestial body around the Earth, its longtitude will be changed over time due to motion of Prime Meridian. So, it is not possible to provide a coordinate system regardless of time for celestial bodies. Instead, Earth-centered inertial (ECI) coordinate systems are used, which remain fixed in space regardless of the Earth's rotation.

Considering an infinite sphere in space with the Earth's center as the origin, the coordinates of celestial bodies can be expressed independently of the Earth's rotation. An observer on Earth can describe the coordinates of a celestial body on this sphere in terms of declination, right ascension, and elevation. The projections of latitudes on this sphere are expressed as declination. The point where the equatorial plane intersects the orbit around the Sun (vernal equinox) is somewhat considered as Greenwich, and the right ascension passing through this point indicates how long it take to observe the celestial body after observing the vernal equinox point. Unlike longitude, right ascension is expressed in hours and minutes, covering one full circle in 24 hours. Elevation is calculated by determining the vertical distance from

the center of the Earth to the celestial body, providing a 3D position relative to the center of the Earth.

2.2. GPS Ephemeris Information

GPS satellites send their positions in the navigation message. The ephemeris information in the navigation message includes the orbital parameters of the satellites around the Earth and their position at a specific moment on this orbit. These parameters are represented by Keplerian parameters which is defined in ECI frame. They can be expressed in three groups.

First group explains the orbit shape of satellite around the Earth. According to Kepler's law, each celestial body has an elliptic orbit shape. For GPS satellites, one of the focal points of orbit is located at Earth's center. Second group defines orientation of the orbit with respect to the Earth's equatorial plane. Third group explains where the satellite is located along its orbit.

2.2.1. Orbit shape

- Eccentricity: Describes how different the elliptical shape is from a perfect circle.
- Semi-Major Axis: The half-length of the axis passing through the ellipse's focal points.

2.2.2. Orbit orientation

- Inclination: The orbit of the satellite and Earth's equatorial plane intersects at two points. The point where the satellite crosses the equatorial plane when it comes from south is defined as right ascension point. The angle at which the satellite's orbit intersects the Earth's equatorial plane in right ascension point is defined as inclination angle.
- Argument of Periapsis: As the satellite progresses along its orbit, after passing the right ascension point, the point where the focal points of its elliptical orbit intersect the major axis is called the perigee point. As the satellite moves away from the Earth after this point, it begins to approach the Earth again after passing this point. The

angle between the perigee point and the right ascension point is defined as the argument of periapsis.

- Longitude of Ascending Node: When the perigee point and the axis passing through the focal points of the satellite's orbit and the center of the Earth are considered, the angle between this axis and the vernal equinox axis is defined as the longitude of ascending node. This parameter is used to determine the orientation of the satellite in space independently of the Earth's rotation around its own axis.

2.2.3. Position of the orbit

- True Anomaly: The angle between the perigee point and the satellite's position on its orbit.

2.3. Coordinate Transformation of Satellite Positions

To calculate the receiver's position from pseudorange equations, the coordinates of the satellites sent in the ECI coordinate system in the navigation message need to be transformed into the ECEF coordinate system that the receiver will use to determine its position. With a couple set of equations, the parameters expressed in ECI frame which is contained in navigation message can be converted to X, Y, and Z coordinates of ECEF reference system.

2.4. Calculating Receiver Position from Pseudorange Equations

GPS satellite orbits are designed so that at least six satellites are visible from any point on Earth. This means that under normal conditions, there are at least six pseudorange equations to calculate the four unknowns on the receiver's side. The number of equations in systems with more equations than unknowns is known as overdetermined systems, and they do not have a solution set. This is also true for the GPS system, where there is no common solution for the X, Y, Z, and time difference unknowns.

Despite the lack of a common solution set for overdetermined systems, various solution methods exist to converge to the most accurate result for all equations. This study investigates the impact of these solution methods on the position accuracy of a GPS receiver.

Eq. 2.1 shows pseudorange equation for one satellite. τ_j represents pseudorange measurement of jth satellite. (x_j, y_j, z_j) mentions satellite coordinates of jth satellite as X, Y, and Z axes, respectively. (x_u, y_u, z_u, δb_u) terms are four unknows of equation which represent X, Y, Z axes coordinates of receiver, and receiver clock bias, respectively. c is speed of light and ε is other error correction terms which affect position accuracy due to previously mentioned error sources.

$$\tau_j = \sqrt{(x_j - x_u)^2 + (y_j - y_u)^2 + (z_j - z_u)^2} + \delta b_u \cdot c + \varepsilon \tag{2.1}$$

Except for ε, which can be calculated using some methods, there are four unknowns for calculating receiver position which are (x_u, y_u, z_u, δb_u). Since pseudorange is measured by subtracting transmit time of signal from satellite and receiving time to receiver, both satellite and receiver have to use common clock. While satellites have atomic clock made of Rubidium and Cesium, receiver clocks are inexpensive and lack the precision required for sensitive measurements. Therefore, receiver clock bias compared to GPS system clock is an unknown for receiver and it must be solved to better estimate of receiver position. To calculate all four unknowns, at least four different pseudorange equations are needed. In other words, at least four different GPS satellites are needed to determine receiver position. GPS satellite constellation is well designed to serve simultaneously all the Earth surface at any time and a receiver in an open environment can observe at least six satellite. The simulation in [28] shows that a receiver may observe up to twelve satellites at the same time over 24 hours period. This means that the receiver must deal with up to twelve pseudorange equations in consideration four unknowns to solve receiver position. This situation leads to not obtaining an exact solution and such of these problems are defined as overdetermined systems in literature [29].

Nevertheless, different methods are developed to estimate most probable solution. In this study, estimation results by the least squares, the weighted least squares and the multilateration methods are compared by means of their position accuracies. Exponential and sigma models are used individually to set weight matrix in weighted least squares method and their result are presented separately. Observation and navigation RINEX (Receiver Independent Exchange Format) files from open platform are used as data sources [30,31]. This open platform has measurements from stationary GPS receiver stations which

their coordinates are known accurately and shared as “approximate position” in RINEX observation files, so that coordinate has taken as reference receiver position to find positional deviation of the results obtained from different position estimation algorithms. RINEX files are resolved in a MATLAB code, then code is utilized to compare mentioned position estimation algorithms [32]. The sigma-modeled weighted least squares method demonstrated its superiority among other algorithms by estimating position with lowest average error for same data.

3. RECEIVER POSITION ESTIMATION METHODS

While GPS receiver has satellite positions and pseudorange measurements, it would be so handy if more precise position accuracy of overdetermined problem is obtained by just doing math. This provides us to improve quality of receiver position accuracy with no cost. How position estimation is processed by three methods is investigated in this section.

3.1. Least Squares Method

The method of least squares provides an approximate solution for overdetermined systems. If this method is applied to the equations in the system, the sum of the squares of the resulting error amounts is the smallest possible value for the system's solution. Thus, the error amounts are distributed with the lowest possible share to all equations, resulting in an approximate solution set.

The method of least squares is only applied to linear systems. Since the pseudorange equations are not linear, linearization processes are required to apply this method. As the first step of the linearization process, an estimate is made for the receiver's position. The estimated receiver's position is expressed as the estimated position in the X-axis ($\widehat{x_u}$), in the Y-axis ($\widehat{y_u}$), in the Z-axis ($\widehat{z_u}$), and the estimated time difference ($\widehat{\delta b_u}$) in Eq. 3.1.

$$\widehat{\alpha_u} = (\widehat{x_u}, \widehat{y_u}, \widehat{z_u}, \widehat{\delta b_u})^T \tag{3.1}$$

According to this estimate, the pseudorange equation can be written as follows. This equation is a function of the $\widehat{\alpha_u}$ matrix which is expressed in Eq. 3.2.

$$\tau_j = f(\alpha_u) = f(x_u, y_u, z_u, \delta b_u) \tag{3.2}$$

The relationship between estimated and the real receiver's position is expressed with the Eq. 3.3 and Eq. 3.4. α_u represents the real position of the receiver, $\widehat{\alpha_u}$ represents the estimated position of the receiver, and $\Delta\alpha$ represents the difference between the real position and the estimated position of the receiver. α_u is consist of actual user position in the X-axis (x_u), in the Y-axis (y_u), in the Z-axis (z_u), and actual time difference (δb_u) in Eq. 3.4.

$$\alpha_u = \Delta\alpha + \hat{\alpha_u} \tag{3.3}$$

$$\alpha_u = (x_u, y_u, z_u, \delta b_u)^T \tag{3.4}$$

When this equation is expressed as a function, it will appear as Eq. 3.5 and Eq. 3.6:

$$\tau_j = f(\alpha_u) = f(\Delta\alpha + \hat{\alpha_u}) \tag{3.5}$$

$$f(x_u, y_u, z_u, \delta b_u) = f([(\Delta x + \hat{x_u}] + [\Delta y + \hat{y_u}] + [\Delta z + \hat{z_u}] + [\Delta\delta b + \hat{\delta b_u}]) \tag{3.6}$$

The real receiver's position can be expressed as the estimated position, the estimated position difference, and the error difference. Based on this, the function is expanded as a Taylor series in Eq. 3.7. Terms of higher orders are denoted as *HOT*.

$$f(\Delta\alpha + \hat{\alpha_u}) = f(\hat{\alpha_u}) + \frac{d(f(\Delta\alpha))}{d\alpha} \cdot f(\Delta\alpha) + HOT \tag{3.7}$$

In the Taylor series expansion, terms of second order and higher are neglected. Since the matrix of the difference between the estimated receiver's position and the real receiver's position consists of four unknowns, its derivative is taken partially which is expressed in Eq. 3.8, Eq. 3.9, Eq. 3.10, Eq. 3.11, Eq. 3.12, and Eq. 3.13.

$$f(\Delta\alpha + \hat{\alpha_u}) = f(\hat{\alpha_u}) + \frac{\partial(f(\Delta x))}{\partial\hat{x_u}} \cdot \Delta x_u + \frac{\partial(f(\Delta y)}{\partial\hat{y_u}} \cdot \Delta y_u + \frac{\partial(f(\Delta z)}{\partial\hat{z_u}} \cdot \Delta z_u + \frac{\partial(f(\Delta\delta b)}{\partial\hat{\delta b_u}} \cdot \Delta\delta b_u \tag{3.8}$$

$$\frac{\partial(f(\Delta x)}{\partial\hat{x_u}} = \frac{(x_j - \hat{x_u})}{r_j} \tag{3.9}$$

$$\frac{\partial(f(\Delta y)}{\partial\hat{y_u}} = \frac{(y_j - \hat{y_u})}{r_j} \tag{3.10}$$

$$\frac{\partial(f(\Delta z)}{\partial\hat{z_u}} = \frac{(z_j - \hat{z_u})}{r_j} \tag{3.11}$$

$$\frac{\partial(f(\Delta\delta b)}{\partial\widehat{\delta b_u}} = \frac{(\delta b_j - \widehat{\delta b_u})}{r_j} \tag{3.12}$$

$$r_j = \sqrt{(x_j - \widehat{x_u})^2 + (y_j - \widehat{y_u})^2 + (z_j - \widehat{z_u})^2} \tag{3.13}$$

When the calculated partial derivatives are used, the estimated pseudorange equation will appear as in Eq. 3.14.

$$\tau_j = \widehat{\tau_j} + \frac{x_j - x_u}{r_j} \cdot \Delta x_u + \frac{y_j - y_u}{r_j} \cdot \Delta y_u + \frac{z_j - z_u}{r_j} \cdot \Delta z_u + \frac{\delta b_j - \delta b_u}{r_j} \cdot \Delta\delta b_u \tag{3.14}$$

When the fractional terms are shown as a single term, the equation will be as Eq. 3.15 and Eq 3.16.

$$\Delta\tau_j = a_{xj} \cdot \Delta x_u + a_{yj} \cdot \Delta y_u + a_{zj} \cdot \Delta z_u + a_{\delta bj} \cdot \Delta\delta b_u \tag{3.15}$$

$$\Delta\tau_j = \tau_j - \widehat{\tau_j} \tag{3.16}$$

As seen, instead of the pseudorange equation, another equation is created with only the coefficients of the unknowns. When calculating the receiver's position, as many equations as the number of visible satellites will emerge.

Linear equations are equations that can be expressed as Eq. 3.17. If the pseudorange equations are to be expressed in this form, they will appear as Eq. 3.18, Eq. 3.19, and Eq. 3.20.

$$A \cdot x = B \tag{3.17}$$

$$A = \begin{bmatrix} a_{x1} & a_{y1} & a_{z1} & a_{\delta b1} \\ a_{x2} & a_{y2} & a_{z2} & a_{\delta b2} \\ a_{x3} & a_{y3} & a_{z3} & a_{\delta b3} \\ \vdots & \vdots & \vdots & \vdots \\ a_{xj} & a_{yj} & a_{zj} & a_{\delta bj} \end{bmatrix} \tag{3.18}$$

$$x = (\Delta x_u, \Delta y_u, \Delta z_u, \Delta \delta b_u)^T \quad (3.19)$$

$$B = (\Delta \tau_1, \Delta \tau_2, \Delta \tau_3, ..., \Delta \tau_j)^T \quad (3.20)$$

If there are four equations, a common solution set is found. If there are more than four equations, this system is an overdetermined system. In this case, the method of least squares can be used.

First, the transpose of matrix A is multiplied on both sides of the equation as Eq. 3.21 and Eq. 3.22. This operation makes the matrix sizes on both sides of the equation equal, and four equations for four unknowns are obtained.

$$A^T \cdot A \cdot x = A^T \cdot B \quad (3.21)$$

$$A^T = \begin{bmatrix} a_{x1} & a_{x2} & a_{x3} & \dots & a_{xj} \\ a_{y1} & a_{y2} & a_{y3} & \dots & a_{yj} \\ a_{z1} & a_{z2} & a_{z3} & \dots & a_{zj} \\ a_{\delta b1} & a_{\delta b2} & a_{\delta b3} & \dots & a_{\delta bj} \end{bmatrix} \quad (3.22)$$

Using the remaining four equations, the four unknowns are solved as Eq. 3.23, Eq. 3.24, Eq. 3.25, and Eq. 3.26).

$$b_{11} \cdot \Delta x_u + b_{12} \cdot \Delta y_u + b_{13} \cdot \Delta z_u + \quad b_{14} \cdot \Delta \delta b_u = a_{x1} \cdot \Delta \tau_1 + a_{x2} \cdot \Delta \tau_2 + a_{x3} \cdot \Delta \tau_3 + \dots \quad (3.23)$$

$$b_{21} \cdot \Delta x_u + b_{22} \cdot \Delta y_u + b_{23} \cdot \Delta z_u + \quad b_{24} \cdot \Delta \delta b_u = a_{y1} \cdot \Delta \tau_1 + a_{y2} \cdot \Delta \tau_2 + a_{y3} \cdot \Delta \tau_3 + \dots \quad (3.24)$$

$$b_{31} \cdot \Delta x_u + b_{32} \cdot \Delta y_u + b_{33} \cdot \Delta z_u + \quad b_{34} \cdot \Delta \delta b_u = a_{z1} \cdot \Delta \tau_1 + a_{z2} \cdot \Delta \tau_2 + a_{z3} \cdot \Delta \tau_3 + \dots \quad (3.25)$$

$$b_{41} \cdot \Delta x_u + b_{42} \cdot \Delta y_u + b_{43} \cdot \Delta z_u + \quad b_{44} \cdot \Delta \delta b_u = a_{\delta b1} \cdot \Delta \tau_1 + a_{\delta b2} \cdot \Delta \tau_2 + a_{\delta b3} \cdot \Delta \tau_3 + \dots (3.26)$$

As it can be seen, the calculated values here are the values in the $\Delta\alpha$ matrix representing the difference between the real receiver's position and the estimated receiver's position. In the method of least squares, when pseudorange equations emerge, the center of the Earth can be assumed as the initial estimate for the receiver's position. As a result of this estimate, another

estimate closer to the real receiver's position is obtained by adding the $\Delta\alpha$ value to the estimate. In this way, in a few iterations, much closer estimates to the real receiver's position will be put forward.

3.2. Weighted Least Squares Method

The solution set obtained in the least squares method simply takes the average of the measured values. In the weighted method, on the other hand, the aim is to increase the influence of reliable measurements on the solution set [33].

Weighted least squares uses same idea with least squares method. Only difference in algorithm is adding weights to Eq. 3.21. Formula used in weighted least squares is given in Eq. 3.27. Weighting is performed by multiplying both sides by R^{-1} which is inverse of covariance matrix. After this calculation, rest of the process is same as least squares method.

$$A^{T} \cdot R^{-1} \cdot A \cdot x = A^{T} \cdot R^{-1} \cdot B \tag{3.27}$$

A covariance matrix is constructed based on the variance value as shown in Eq. 3.28. Although different approaches have been developed for weighting process, exponential and sigma model weighting based on SNR is used this thesis. There are some models based on elevation angle of visible satellites, however it is shown in [25] that the models based on SNR are yields more reliable solution than the ones based on elevation angle. Variance values can be determined by exponential and sigma weighting models. Both of weighting models take SNR values of each satellite as weights of observation. More SNR value is considered as more reliable observation.

$$R = diag(\sigma_1^2, \sigma_2^2, \dots, \sigma_j^2) \tag{3.28}$$

In the exponential-modeled weighted least squares method, variance values are calculated as Eq. 3.29 where s_j is j^{th} covariance matrix and a, b, k is model parameters. Different values of model parameters are tested in [25] and $a = 0$, $b = 1$ and $k = 0.3$ is determined as optimal condition for exponential model.

$$s_j = a + b \cdot e^{k \cdot (\min(SNR) - SNR_j)} \tag{3.29}$$

In sigma-modeled weighted least squares method, variance values are calculated as Eq. 3.30. Different values of model parameters are tested in [25] and $a = 0$ and $b = 1.e5$ is determined as optimal condition for sigma model.

$$s_j = \sqrt{a + b \cdot 10^{(-SNR_j)/10}} \tag{3.30}$$

The sum of weighted factors is normalized by Eq. 3.31 and weights to be used in Eq. 3.27 are obtained.

$$\sigma_j^2 = s_j / \left(\prod_{j=1}^{N} s_j \right)^{1/N} \tag{3.31}$$

Similar to the least squares method, in the case of the receiver's initial estimate, the center of the Earth is assumed, and after a few iterations, very close estimates to the actual receiver position are determined.

3.3. Multilateration Method

Global positioning systems are generally designed to calculate the receiver's position using a trilateration method. To do this, three satellite distances to receiver are calculate. Three different spheres are created which their center is located at each satellite and their radius is the distance between each satellite to receiver. Three spheres give two intersection point. The point near the Earth is accepted as receiver position as trilateration method. In everyday use scenarios, receivers obtain distances from more than three satellites. Therefore, a common intersection point may not be obtained for more than three spheres, so receiver position cannot be provided. With the multilateration method, an algebraic estimate for the receiver's position is provided without the need for an iteration [27].

If number of observed satellites is only four and nonexistence of other errors, multilateration method brought forward by Bancroft gives true position. For more than four satellites, Moore-Penrose pseudoinversion should be implemented to get more accurate solution [34]. In this method, nx4 data matrix consists of satellite positions and pseudoranges is

constructed as Eq. 3.32 and Eq. 3.33. a_j represents data matrix of j^{th} satellite. *S* matrix keeps data matrixes of observed satellites.

$$S = (a_1, a_2, a_3, \ldots, a_n)^T \tag{3.32}$$

$$a_j = (x_j, y_j, z_j, \tau_j)^T \tag{3.33}$$

Bancroft utilize Minkowski sum to implement a solution for overdetermined problem. Formulation of Minkoswki is shown in Eq. 3.34. It is applied to data matrixes of all observed satellites and construct *r* matrix as Eq. 3.35 and Eq. 3.36. r_j represents half of Minkowski sum for j^{th} satellite.

$$\langle a, b\rangle = a_1 \cdot b_1 + a_2 \cdot b_2 + a_3 \cdot b_3 - a_4 \cdot b_4 \tag{3.34}$$

$$r_j = \langle a_j, a_j\rangle / 2. \tag{3.35}$$

$$r = (r_1, r_2, r_3, ..., r_n)^T \tag{3.36}$$

H matrix of generalized inverse function is calculated as Eq. 3.37. If so, any weight is known, this *H* matrix can be modified with weights. However, it is not covered in this study.

$$H = (S^T \cdot S)^{-1} \cdot S^T \tag{3.37}$$

E, *F* and *G* coefficients are calculated as Eq. 3.38, Eq. 3.39, and Eq. 3.40. *u* and *v* parameters are defined in Eq. 3.41 and Eq. 3.42. i_0 identity matrix to calculate *u* shown in Eq. 3.43.

$$E = \langle u, u\rangle \tag{3.38}$$

$$F = \langle u, v\rangle - 1 \tag{3.39}$$

$$G = \langle v, v\rangle \tag{3.40}$$

$$u = H \cdot i_0 \tag{3.41}$$

$$v = H \cdot r \tag{3.42}$$

$$i_0 = (1, 1, 1, ..., 1)^T \tag{3.43}$$

E, *F* and *G* coefficients used to calculate roots of λ which is in Eq. 3.44.

$$E \cdot \lambda^2 + 2 \cdot F \cdot \lambda + G = 0 \tag{3.44}$$

Eq. 3.44 provides two roots for λ which are $\lambda_{1,2}$. Column vectors in Eq. 3.45 is calculated using these roots, $y_{1,2}$.

$$y_{1,2} = \lambda_{1,2} \cdot u + v \tag{3.45}$$

The vector *y* gives *x* user position and *b* receiver clock offset as Eq. 3.46. Although there are two solutions for Eq. 3.45, actual solution can be determined by checking the user position solution via pseudorange equation in Eq. 2.1.

$$y^T = (x^T - b)^T \tag{3.46}$$

4. TEST SETUP AND RESULTS

In the context of this thesis, it is aimed to compare three different estimation method. RINEX files is processed in MATLAB and analyzed.

4.1. RINEX Navigation and Observation Files

Position estimation methods require satellite positions in view and pseudorange measurements of each satellite to receiver. RINEX data format provides this information. RINEX files is commonly accepted as a standard and various institution in the world is present their hourly or daily datasets in this format. IGS and RCTM (Radio Technical Commission for Maritime Services) are responsible for updating and maintaining the RINEX format to meet the needs of the IGS and the GNSS Industry. IGS distributes older and last versions of the RINEX standard freely in [35]. The satellite positions are acquired from RINEX navigation file and pseudorange measurements from RINEX observation file [30, 31].

RINEX observation file stores pseudorange measurements for visible satellites to user along with some error corrections measurements to compensate errors like ionospheric and tropospheric delays. It can be dealed with in two parts, the header section, and the measurements section. Bislin made a clear explanation and demonstration about how the RINEX observation data is read on his blog [36]. Figure 4.1. shows the header part and just two measurements of observation of a RINEX observation file.

In the header area of observation file, there are a lot of useful information about the observation and the station. RINEX version, measurement time, the satellites observed during measurement, antenna type of the receiver are a few contents of the file. The row of "# / TYPES OF OBSERV" is colored and explained with ease in Figure 4.1. In the mentioned example, this row clarifies that observation consists of 5 different types, C1, C2, L1, L2, and P2. The observations in the second section from each type is shown in Figure 4.1. Executive institution of stationary GPS station provides receiver position as "Approximate position XYZ" in WGS84 ECEF coordinates. This position is accepted as

true reference value for the output of three different position estimation methods under investigation.

RINEX navigation file stores ephemeris data which is broadcasted in the same content from all satellites. Ephemeris data is structure of satellite positions in all GPS orbits and this data uses Keplerian parameters to define satellite positions. Since ephemeris data is accepted to be valid for two minutes, RINEX navigation file keeps ephemeris data within two minutes period. It should not be forgotten that before defining these parameters to position estimation algorithms, correction of Earth rotation must be performed to satellite positions.

Similar to observation file, RINEX navigation file consists of header and measurement sections. In the header section, the user is informed about RINEX version, RINEX type, measurement time, ionospheric corrections etc.

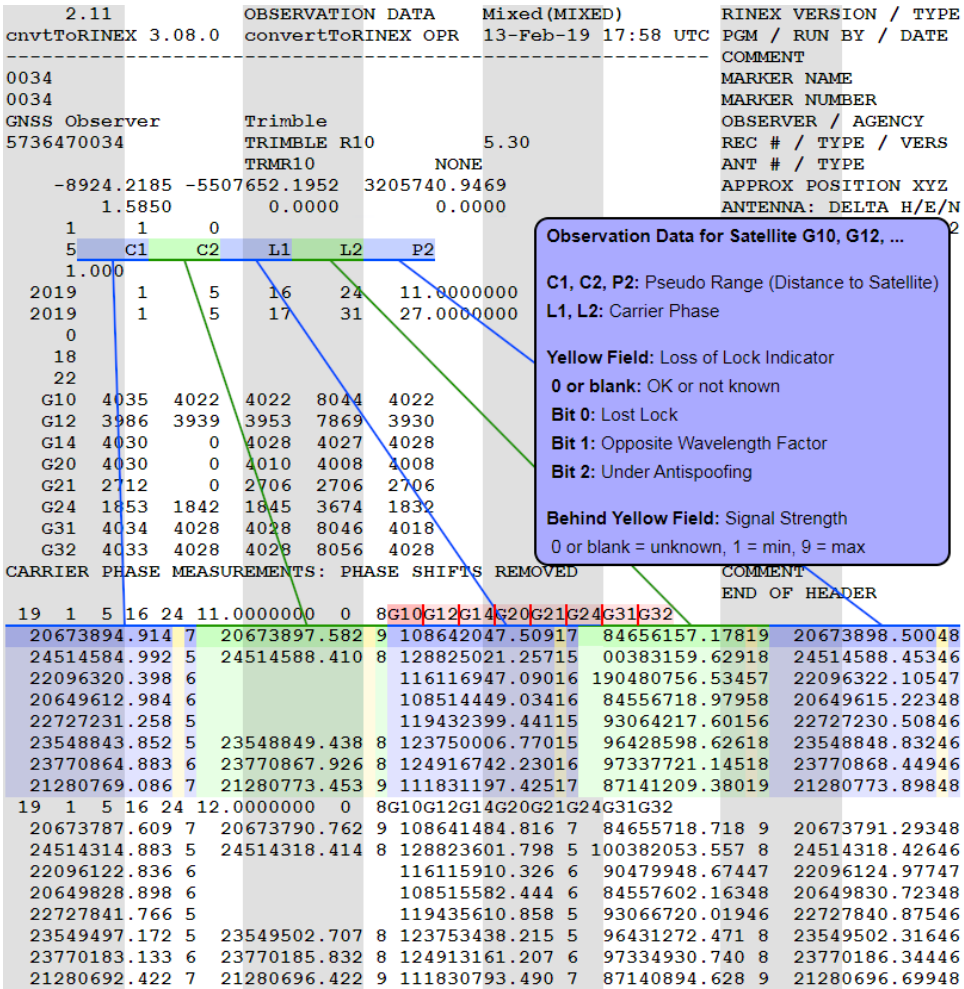

Figure 4.1. The demonstration of some coloumns in RINEX observation file [36]

4.2. MATLAB Code

MATLAB code of [32] is used to read RINEX files with some corrections and additions, like making it suitable to read RINEX 3 observation files. For multilateration method, MATLAB code of [37] is provided to implement the method. The code firstly performs ionospheric and tropospheric corrections to pseudorange measurements following by correction of Earth rotation to satellite positions. Then, the code is implemented which includes three different position estimation methods and their comparison of reference receiver position. For least squares and weighted least squares methods, five iterations are performed for each measurement. The code is utilized and designed flexible to perform as much as the number of desired epochs. The used MATLAB code is uploaded to GitHub, and it is accessible on [38].

4.3. The Reference GPS Station

To present at this thesis, observation, and navigation RINEX files from AMC400USA station of IGS (International GNSS Service) network is chosen. AMC stands for Alternate Master Clock. This station is located near Colorado Springs, USA which is shown in Map 4.1. The fixed stations of IGS network have ability to measure their locaitions so precisely that, for example, the fixed station in Ankara measured about 6 mm displacement during the earthquake happened in the south-eastern of Turkey on February 6, 2023 [39].

Both observation and navigation RINEX files are generated on January 31, 2023, and observation file contains information of 30 seconds period while navigation file has two minutes period [30, 31]. First few measurements and header sections of obervation and navigation RINEX files are presented in APPENDIX-1 and APPENDIX-2, respectively.

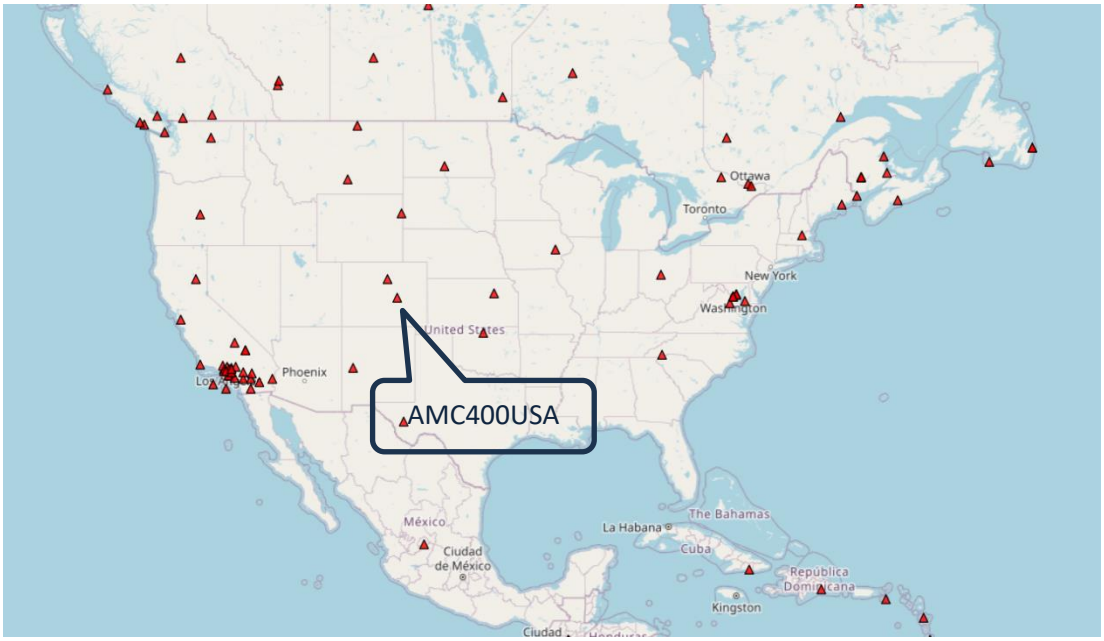

Map 4.1. The location of AMC400USA station

4.4. Determining Weights for WLS Method

SNR values which are taken as weight are obtained from S1 and S2 parameters of observations file. Exponential and sigma weighting models are used to get weighted least squares solution. While both models are utilized for taking SNR measurements to determine weights, their variance calculations are slightly different. Variance calculation of exponential model is given in Eq. 3.29 and variance calculation of sigma model is given in Eq. 3.30. The coefficients in these calculations were analyzed in [25]. For exponential model, $a = 0$, $b = 1$ and $k = 0.3$ were the best values. For sigma model, $a = 0$ and $b = 1.e5$ were the best values. These recommended values are rechecked to look forward a better result as a part of this study. Then, different coefficients are tested if another weighting calculation gives better solution.

4.4.1. Coefficients for exponential modeled WLS

Figure 4.2. shows mean error of different model parameters in the exponential modeled weighted least squares method for each epoch. Figure 4.3., Figure 4.4. and Figure 4.5. shows errors in each axis for each epoch. These figures are recorded for 3 000 seconds. Since each observation is made within 30 seconds, totally 100 measurements are compared.

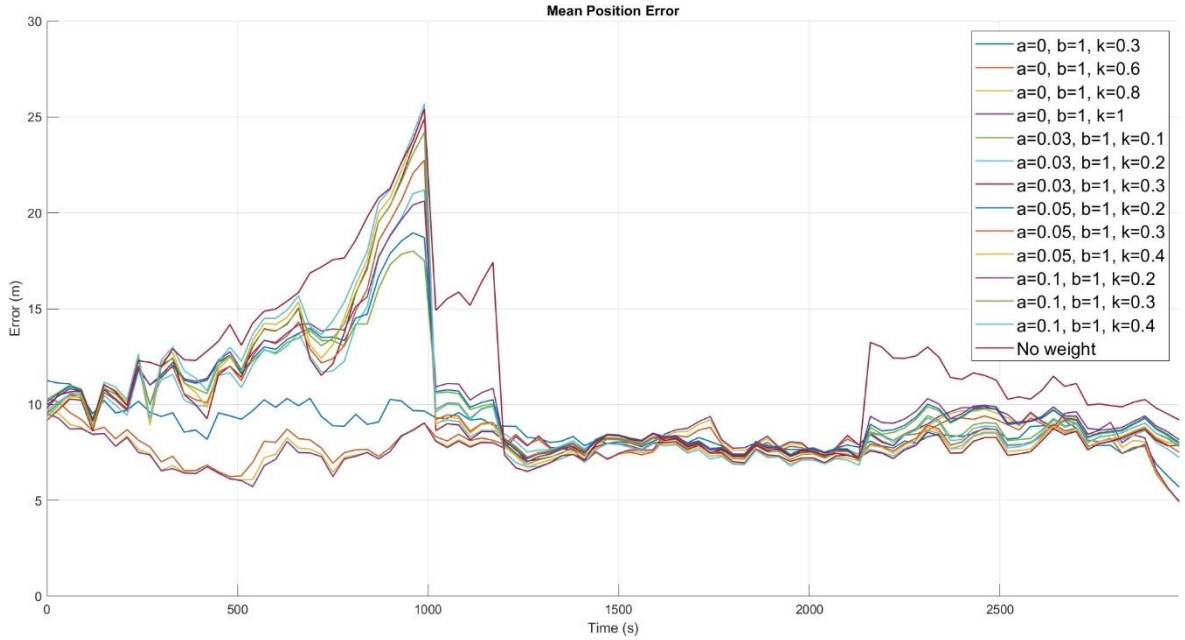

Figure 4.2. Mean error of different model parameters in exponential model for each epoch

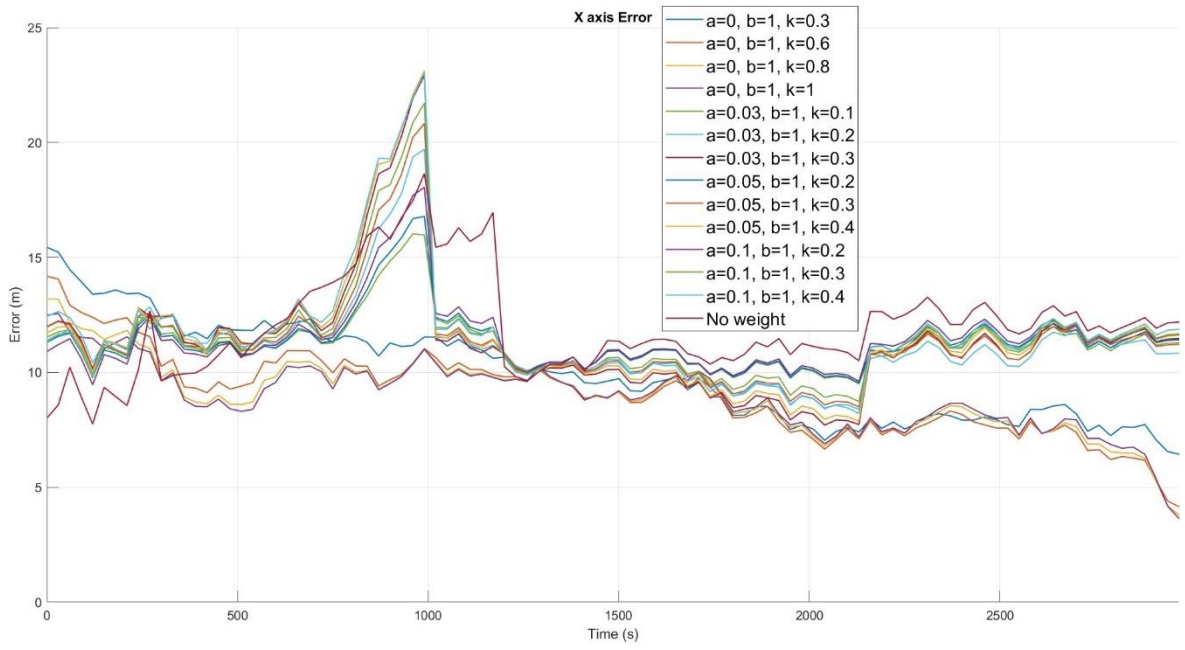

Figure 4.3. X axis error of different model parameters in exponential model for each epoch

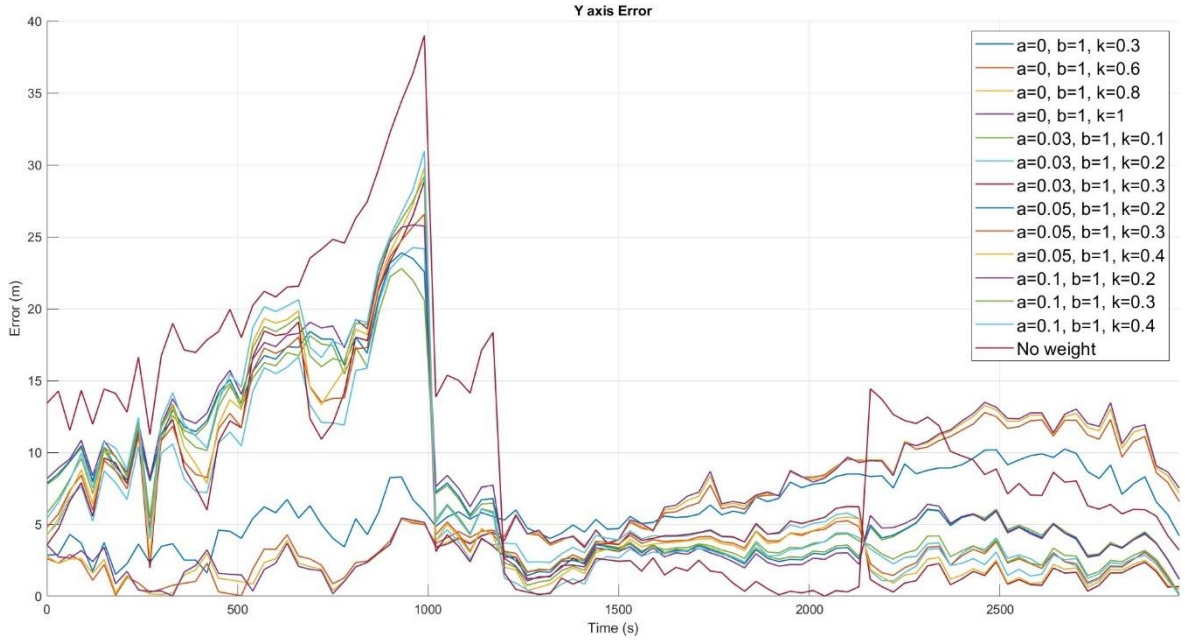

Figure 4.4. Y axis error of different model parameters in exponential model for each epoch

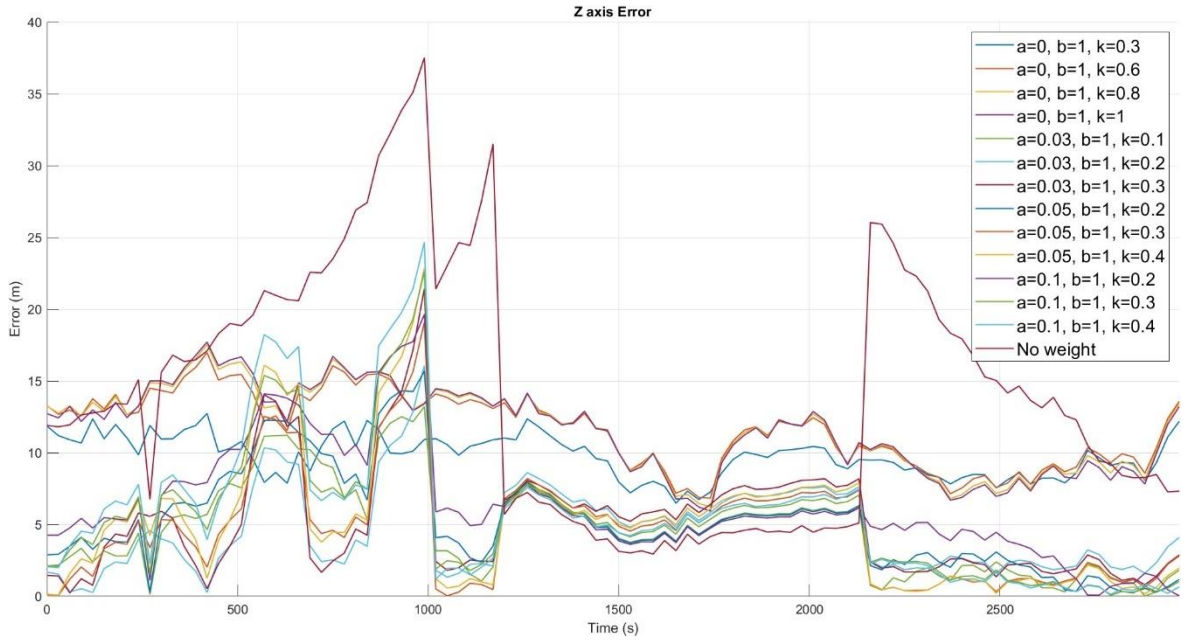

Figure 4.5. Z axis error of different model parameters in exponential model for each epoch

Table 4.1. shows average error and mean errors in each axis of different model parameters used in exponential modeled weighted least squares method. It summarizes figures which presents errors in each epoch and basically takes average of whole measurements. These results implies that best model parameters which provides least mean error is acquired when $a = 0$, $b = 1$ and $k = 0.8$ is chosen.

Table 4.1. Errors of different model parameters for exponential model

	Average Error (m)	X Axis Mean Error (m)	Y Axis Mean Error (m)	Z Axis Mean Error (m)
a = 0, b = 1, k = 0.3	8.66	9.92	6.14	9.77
a = 0, b = 1, k = 0.6	8.01	9.05	5.92	11.67
a = 0, b = 1, k = 0.8	7.97	8.94	6.03	11.72
a = 0, b = 1, k = 1	7.99	8.91	6.14	11.66
a = 0.03, b = 1, k = 0.1	9.98	11.28	7.37	4.66
a = 0.03, b = 1, k = 0.2	9.58	11.19	6.36	4.57
a = 0.03, b = 1, k = 0.3	9.68	11.35	6.33	5.05
a = 0.05, b = 1, k = 0.2	10.05	11.34	7.49	5.17
a = 0.05, b = 1, k = 0.3	9.76	11.32	6.64	4.57
a = 0.05, b = 1, k = 0.4	9.84	11.46	6.60	5.03
a = 0.1, b = 1, k = 0.2	10.23	11.45	7.78	6.21
a = 0.1, b = 1, k = 0.3	10.04	11.50	7.14	5.40
a = 0.1, b = 1, k = 0.4	10.10	11.62	7.07	5.70
No weight	11.54	11.94	10.76	13.99

4.4.2. Coefficients for sigma modeled WLS

Figure 4.6. shows mean error of different model parameters in the sigma modeled weighted least squares method for each epoch. Figure 4.7., Figure 4.8. and Figure 4.9. shows errors in each axis for each epoch. These figures are recorded for 3 000 seconds. Since each observation is made within 30 seconds, totally 100 measurements are compared.

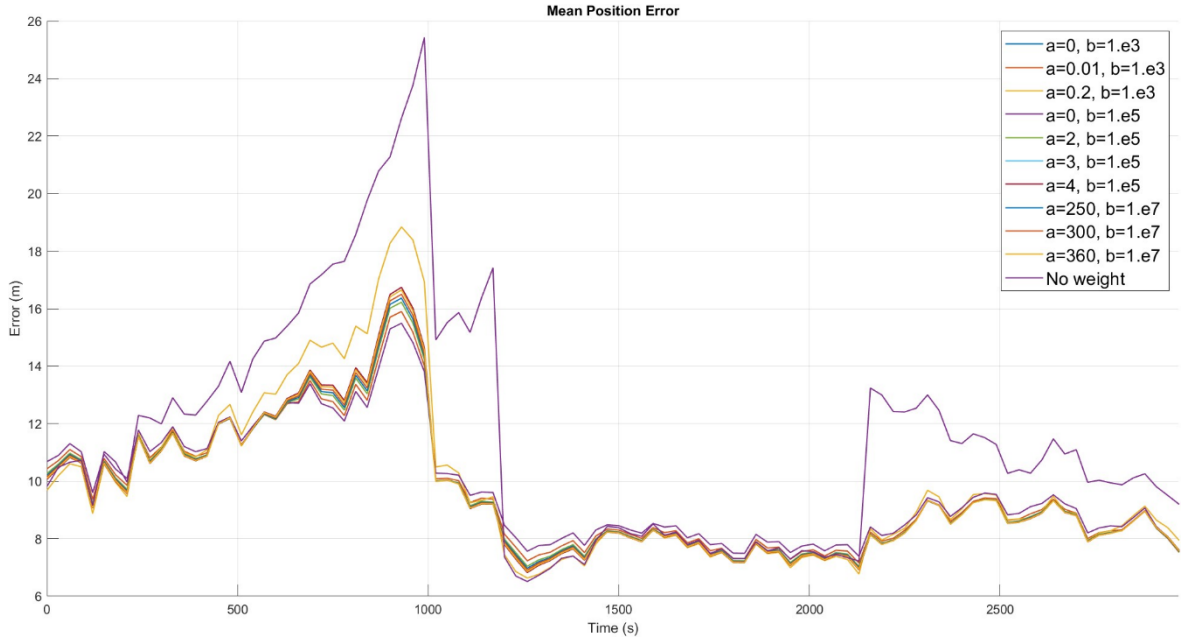

Figure 4.6. Mean error of different model parameters in sigma model for each epoch

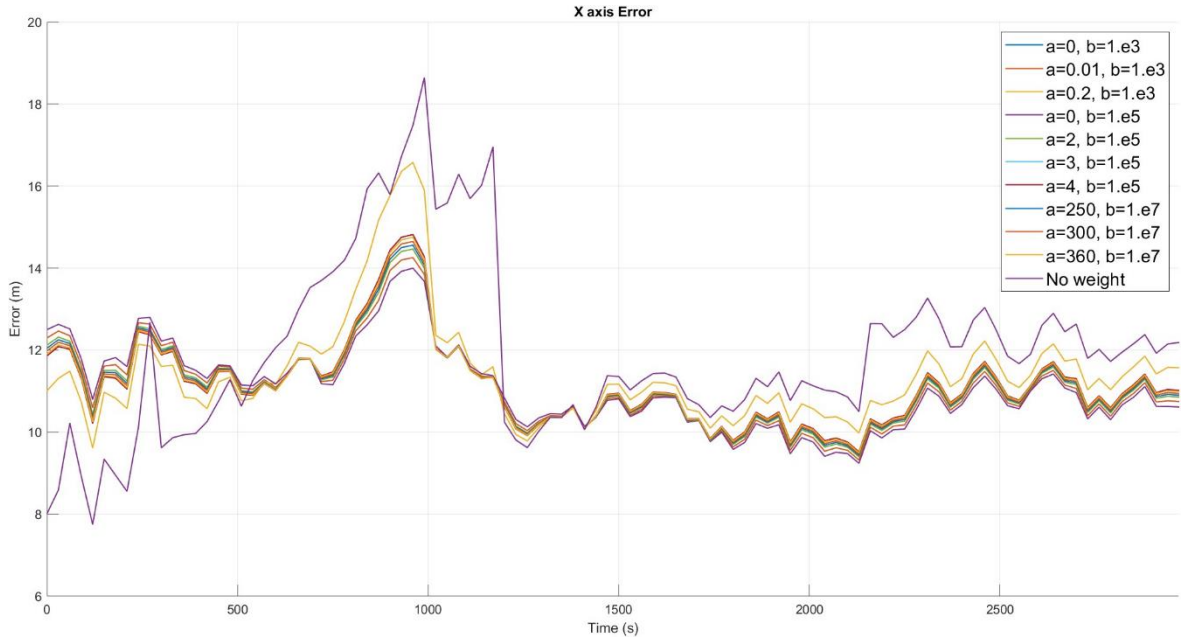

Figure 4.7. X axis error of different model parameters in sigma model for each epoch

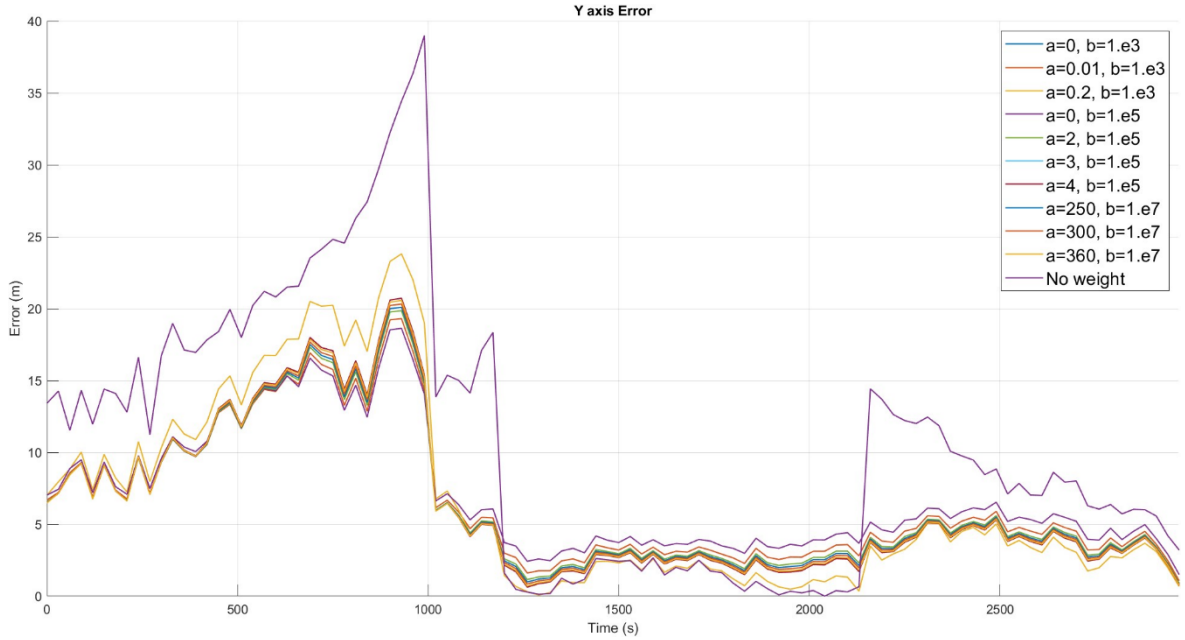

Figure 4.8. Y axis error of different model parameters in sigma model for each epoch

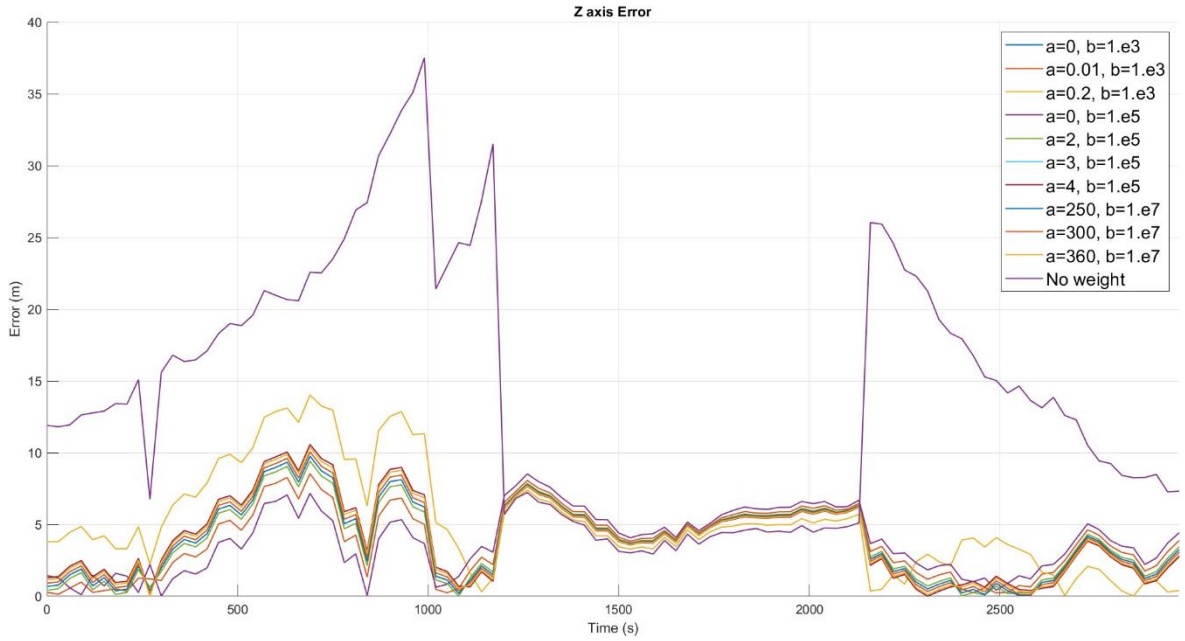

Figure 4.9. Z axis error of different model parameters in sigma model for each epoch

Table 4.2. shows average error and mean errors in each axis of different model parameters used in sigma modeled weighted least squares method. These results implies that best model parameters which provides least mean error is acquired when $a = 3$ and $b = 1.e5$ is chosen.

Table 4.2. Errors of different model parameters for sigma model

	Average Error (m)	X Axis Mean Error (m)	Y Axis Mean Error (m)	Z Axis Mean Error (m)
a = 0, b = 1.e3	9.73	11.06	7.05	3.82
a = 0.01, b = 1.e3	9.60	11.08	6.63	3.80
a = 0.2, b = 1.e3	9.84	11.42	6.66	5.13
a = 0, b = 1.e5	9.73	11.06	7.05	3.82
a = 2, b = 1.e5	9.56	11.11	6.47	3.86
a = 3, b = 1.e5	9.55	11.13	6.39	3.97
a = 4, b = 1.e5	9.56	11.16	6.36	4.06
a = 250, b = 1.e7	9.56	11.12	6.43	3.92
a = 300, b = 1.e7	9.55	11.13	6.39	3.97
a = 360, b = 1.e7	9.56	11.15	6.37	4.02
No weight	11.54	11.94	10.76	13.99

4.5. Comparison of Different Methods

Figure 4.10. shows mean error of different position estimation methods for each epoch. Figure 4.11., Figure 4.12. and Figure 4.13. shows errors in each axis for each epoch. These figures are recorded for 3 000 seconds. Since each observation is made within 30 seconds, totally 100 measurements are compared.

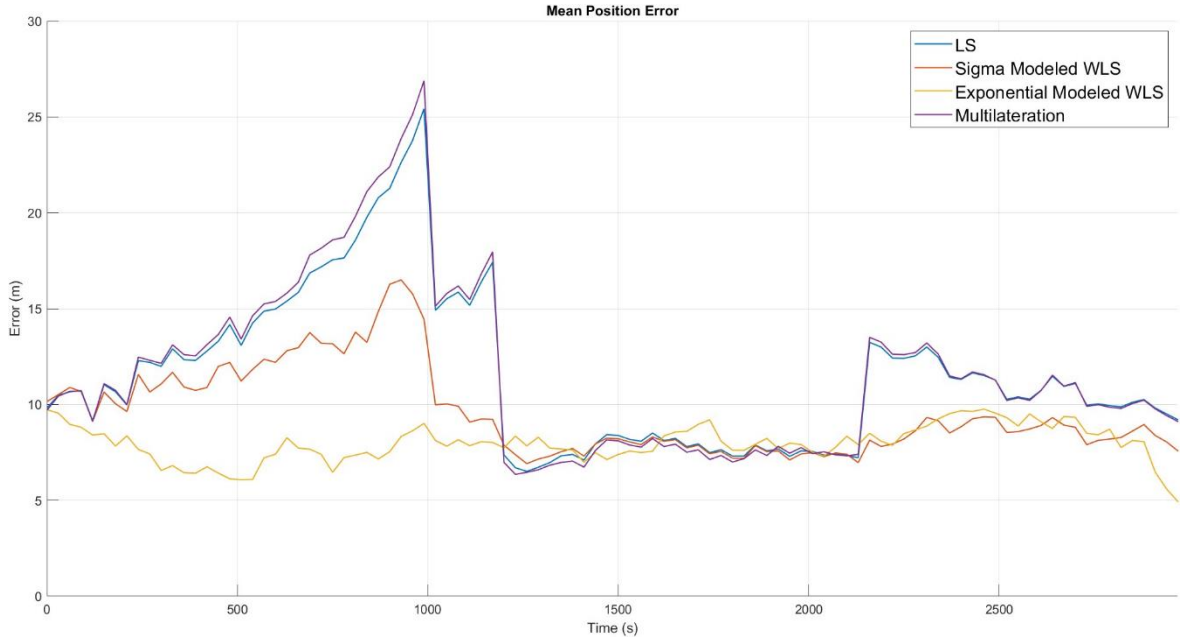

Figure 4.10. Mean position error of different estimation methods for each epoch

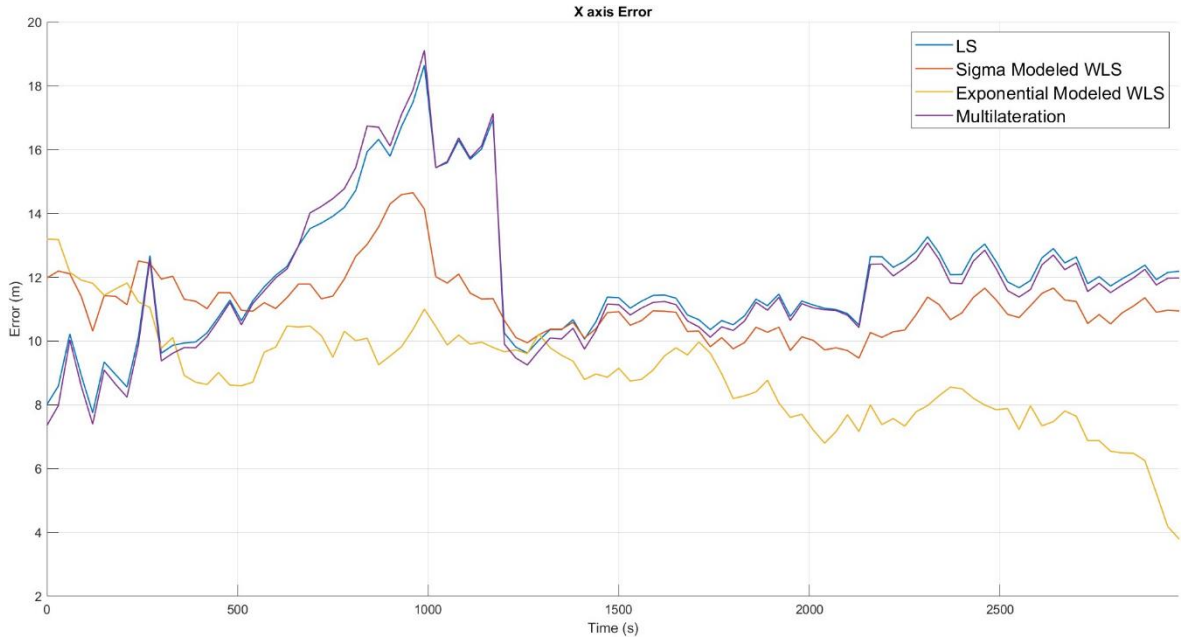

Figure 4.11. X axis position error of different estimation methods for each epoch

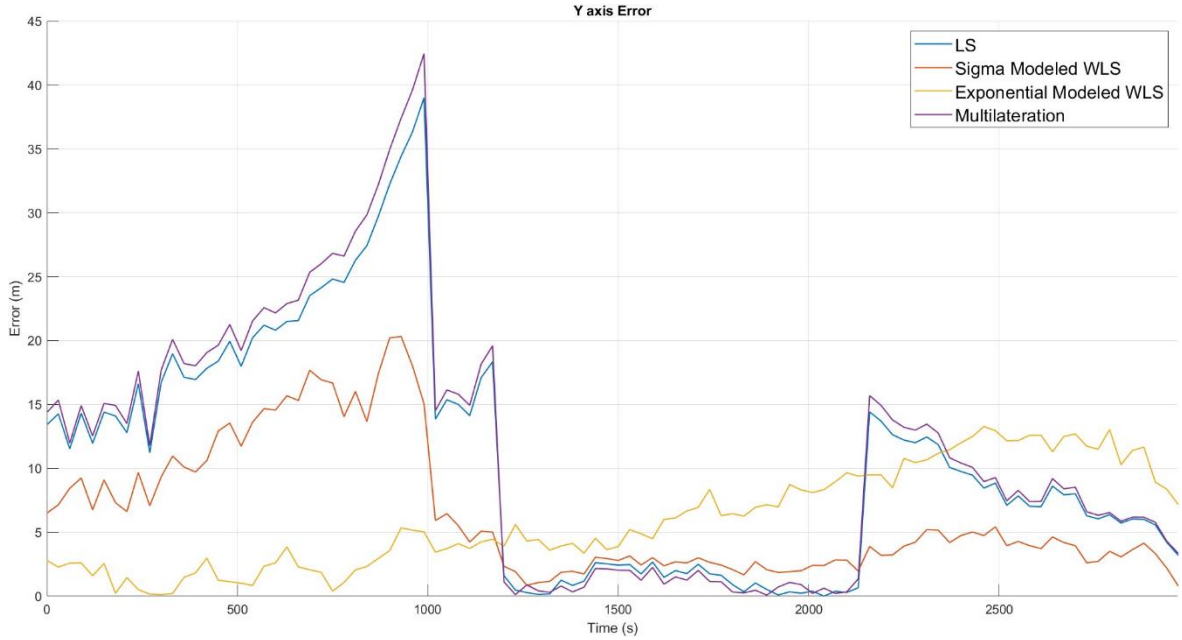

Figure 4.12. Y axis position error of different estimation methods for each epoch

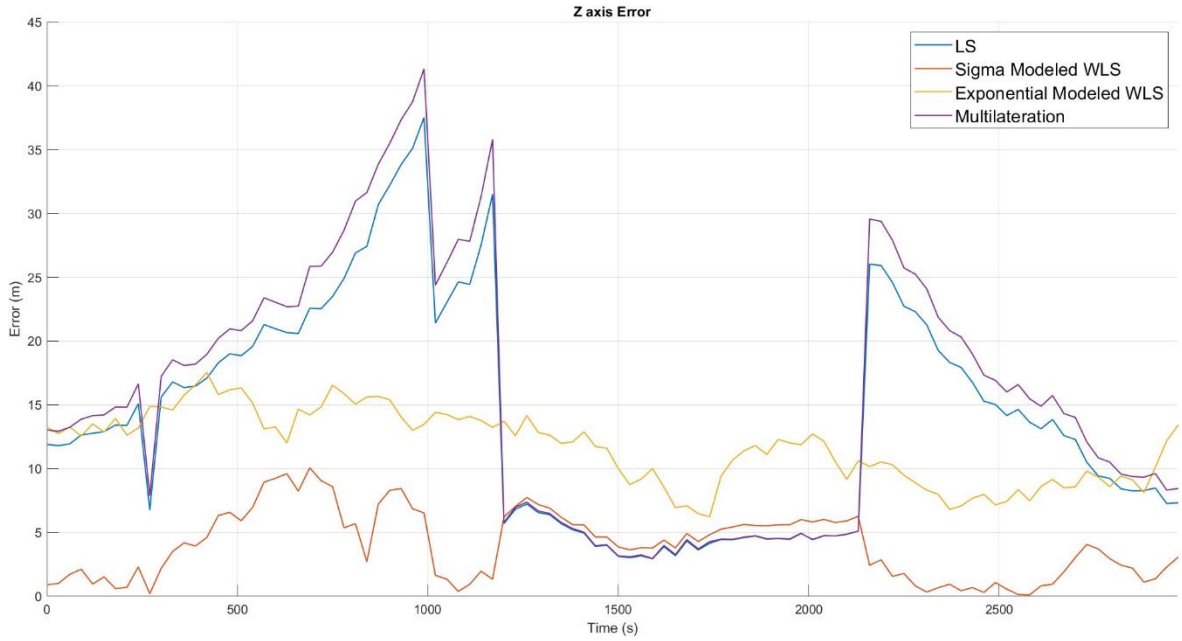

Figure 4.13. Z axis position error of different estimation methods for each epoch

Table 4.3. shows errors of each method after averaging over 100 samples. It includes total mean error in addition to separately calculateded errors in X, Y and Z axis. As seen mean error in Table 4.3., exponential modeled weighted least squares method provided least position error.

Table 4.3. Comparison of position errors for estimation methods

	Average Error (m)	X Axis Mean Error (m)	Y Axis Mean Error (m)	Z Axis Mean Error (m)
Least Squares Method	11.54	11.94	10.76	13.99
Exponential-modeled Weighted Least Squares Method	7.97	8.94	6.03	11.72
Sigma-modeled Weighted Least Squares Method	9.55	11.13	6.39	3.97
Multilateration Algebraic Method	11.69	11.82	11.42	15.56

5. DISCUSSION

In this thesis, least squares method, weighted least squares method, and multilateration method are compared in terms of positioning errors. In the weighted least squares method, exponential and sigma models are used to determine weights. Different values are tried for the coefficients used in these models, and the coefficients providing the least position error are investigated. These coefficients show very little difference compared to other studies in the literature.

In [25], conference paper explained that the optimal values for the coefficients in exponential model are presented as $a = 0$, $b = 1$, and $k = 0.3$ so that the solution yields least mean positioning error. However, in the study conducted within the scope of the thesis, the optimal values are calculated as $a = 0$, $b = 1$ and $k = 0.8$. The variation in optimal model parameters highlights the challenge of developing a model that performs effectively across diverse environments. The model determines how much weight should given to each measurement. Because the model is only based on SNR values, other factors which effect the relialibility of measurements is ignored. So, the difference between thesis study and [25] may showed up because of other factors.

In [25], mean positioning error is increased while a variable is scaled up and k variable is kept constant. If k variable is scaled up beginning from zero and a variable kept constant, mean position error converges until an uncertain point. Then, it begins to diverge. In the study within the scope of this thesis, changes in position estimation error depending on a and k variables occurred similarly.

The coefficients used in the sigma model are decided as $a = 0$ and $b = 1.e5$ to minimize the position error in [40]. In the study conducted within the scope of this thesis, $a = 3$ and $b = 1.e5$ values are found which yields least mean positioning error. Same arguments mentioned for exponential model is valid for the sigma model. The difference between thesis study and [40] may showed up because of other factors.

Exponential modeled weighted least squares method which yields 7.97 meters error on average provides best estimate among other methods. In the thesis study, a 31% reduction

in average positioning error is observed with exponential model and 17% error reduction with sigma model weighted least squares solution compared to the least squares method. Average positioning error is corrected up to 10% using exponential modeled and 7% using sigma modeled weighted least squares method compared to least squares method in [25]. On the other hand, average positioning error is enhanced 49% using sigma modeled weighted least squares method compared to least squares in [40]. The results for thesis are between the ones in literature. In addition, the thesis study showed that multilateration method yields 1% worse estimation with respect to least squares.

The variation in position estimation errors on the X, Y and Z axes has been investigated separately within the thesis, too. Although weighted least squares method with the exponential model has resulted in lower average position errors, the difference of mean errors in Z axis deserves to mention. Sigma modeled weighted least squares method provides best solution in Z axis with 3.97 meters average error. This result is 66% better than exponential modeled weighted least squares. In the thesis study, sigma model decreased the mean error at a rate of 7% in X axis, 41% in Y axis and 72% in Z axis. In [40], sigma model weighted least squares method enhanced the mean accuracy of estimate at a rate of 41% in Y axis, 70% in Z axis while a deteoration is observed at a rate of 86% in X axis. The results for each axis contradict when it comes to X axis. It was expected to see same enhancements in X axis for the study in [40], however the environmental conditions and receiver hardware may affect the result.

6. CONCLUSION

In this thesis, three different position estimation methods used in the solutions of GPS pseudorange equations, namely least squares, weighted least squares, and multilateration methods, were compared to investigate which one of them provides better position accuracy. Exponential and sigma weighting models were used for weighted least squares method. Positon estimation methods take the satellite positions and pseudorange measurements, then they yield receiver position after processing data in their own ways. A fixed GPS station was selected for test and simulation. This station publishes online its measurements and its certain coordinate on Earth as RINEX files. Satellite positions was obtained from observation file and pseudorange measurement was obtained from navigation file from this station. A MATLAB code was utilized to scan and separate required information from RINEX files. Then, same MATLAB code was used to process position estimation methods. All methods had same inputs as satellite positions and pseudorange measurements, however they gave different position estimations. Effectiveness of three different position estimation methods is compared by the difference to the real location of the fixed station.

This thesis showed that weighting based on SNR improves position estimation accuracy significantly. Exponential model weighted least squares methods estimates receiver position 31% more precisely than least squares method. Sigma model weighted least squares methods enhances the positioning accuracy at a rate of 17% compared to least squares method. On the other hand, multilateration method makes the estimation only 1% worse compared to least squares method.

Least squares method is widely used in industry and became a basic approach of position estimation. However, each visible satellite can not provide data at the same reliability. The signals of satellites can exposure to different amounts of environmental impacts. For example, the signal from a satellite at horizon spends more time in ionosphere and troposphere compared to a satellite at the zenith of the receiver. Weighted least squares method recommends a solution which give more emphasis to reliable measurements. This method is applied in some advanced receivers and there are lots of studies on how weighting can be done. This thesis will contribute to the literature about how to determine weights and explore the impacts of weighting solution.

While least squares and weighted least squares methods requires iteration, multilateration method estimates position via algebraic calculation. This thesis showed that this method is relatively realiable and can be preferred in the absence of smart devices.

The statistical test results are detailed and compared with previous research in literature in “Discussion” section. Test results are generally consistent with the studies in literature. However, the measurements and processing the data may leads to differences in solutions. For example, it is not known that how good multipath errors are eliminated in other studies. Thus, model parameters in weighted least squares method in the thesis study are slightly different from the recommended values in some literature sources. In another perspective, the differences between thesis study and literature sources concludes that it is difficult to create a weighing model without considering or eliminating other error sources. Thus, it can be said that it is hard to implement theoretical suggestions to practical solutions unless all medium and environmental impacts are thoroughly analyzed.

For the future works, same methods and same model parameters may be implemented with different GPS data to see the weighting model is consistent. Different weighting model based on alternative properties may be investigated. Coefficients in known weighting model may be examined to determine the optimum values via artificial intelligence. Initial values in least squares and weighted least squares methods may be considered to reach the solution faster or to acquire a better estimation. The estimation of multilateration mehod may be used as the initial condition of least squares and weighted least squares methods.

REFERENCES

1. Internet: The Aerospace Corporation. (n.d.). Brief history of GPS. URL: https://aerospace.org/article/brief-history-gps# Last Accessed on October 20, 2023.

2. Internet: Hurley, S. (2017, January 29). GPS. URL: https://explainingscience.org/2017/01/29/gps/ Last Accessed on October 25, 2023.

3. Borre, K., Akos, D., Bertelsen, N., Rinder, P., Jensen, S. (2007). *A software-defined GPS and Galileo receiver: A single-frequency approach.* (1 ed.). Boston, Basel, Berlin: Birkhauser, 101-105.

4. Hegarty, C., Kaplan, E. (2005). *Understanding GPS principles and applications.* (2 ed.). Boston, London: Artech House, 295-300.

5. Internet: Rathore, C. S. (2017, February 16). Plannig a GPS survey part 2 - Dilution of precision errors. URL: https://graticules.blogspot.com/2017/02/planning-gps-survey-part-2-dilution-of.html Last Accessed on September 18, 2023.

6. Zhao, L., Li, L., Zhao, X. (2009). *An adaptive hatch filter to minimize the effects of ionosphere and multipath for GPS single point positioning.* 2009 International Conference on Mechatronics and Automation, Changchun, China, 4167-4172.

7. Sukcharoen, T., Wu, F., Weng, J. (2015). *Characteristics of ionosphere at equatorial and middle latitude zones during solar maximum.* 2015 12th International Conference on Electrical Engineering/Electronics, Computer, Telecommunications and Information Technology (ECTI-CON), Hua Hin, Thailand, 1-6.

8. Akiyama, N., Tanaka, T., Yonekawa, M. (2007). *Improvement of GPS positioning accuracy by ionosphere delay correction*. SICE Annual Conference 2007, Takamatsu, Japan, 1766-1769.

9. Guo, J., Yang, F., Shi, J., Xu, C. (2016, December). An optimal weighting method of Global Positioning System (GPS) troposhere tomography. *IEEE Journal of Selected Topics in Applied Earth Observations and Remote Sensing*, 9(12), 5880-5887.

10. Wang, C., Liou, Y., Yeh, T. (2007). *The impact of surface meteorological measurements on GPS height determination.* 2007 IEEE International Geoscience and Remote Sensing Symposium, Barcelona, Spain, 2959-2962.

11. Koohzadi, M., Ebadollahi, S., Vahidnia, R., Dian, F. J. (2019). *Implementation and comparison of different troposheric models to reduce error low-cost real-time GPS positioning.* 2019 IEEE 10th Annual Information Technology, Electronics and Mobile Communication Conference (IEMCON), Vancouver, BC, Canada, 82-86.

12. Hofmann-Wellenhorf, B., Lichtenegger, H., Wasle, E. (2007). *GNSS – Global Navigation Satellite Systems: GPS, GLONASS, Galileo and more*. (1 ed.). Wien, New York: Springer Science & Business Media, 105-111, 154-160, 262-265.

13. Rlinami, M., Morikawa, H., Aoyama, T. (2000). *An adaptive multipath mitigation technique for GPS signal reception.* 2000 51st Vehicular Technology Conference Proceedings, Tokyo, Japan, 2, 1625-1629.

14. Phan, Q., Tan, S. (2011). *Mitigation of GPS periodic multipath using nonlinear regression.* 2011 19th European Signal Processing Conference, Barcelona, Spain, 1795-1799.

15. Kim, S., Lee, H., Park, K. (2021). *GPS multipath detection based on carrier-to-noise-density ratio measurements from dual-polarized antenna.* 2021 21st International Conference on Control, Automation and Systems (ICCAS), Jeju, Korea, Republic of., 1099-1103.

16. Ashby, N. (2003, January 28). Relativity in the Global Positioning System. *Living Reviews in Relativity*, 6(1), 5-10.

17. Ashby, N. (2002, May). Relativity and Global Positioning System. *Physics Today*, 55(5), 41-47.

18. Internet: NASA. (2020, October 22). Relativity in the Global Positioning System - Einstein's theory of relativity, critical for GPS, seen in distant stars. URL: https://www.nasa.gov/image-article/einsteins-theory-of-relativity-critical-gps-seen-distant-stars/ Last Accessed on October 25, 2023.

19. Internet: Pogge, R. (2017, March 11). Real-world relativity: The GPS navigation system. URL: https://www.astronomy.ohio-state.edu/pogge.1/Ast162/Unit5/gps.html#note02 Last Accessed on October 26, 2023.

20. Wang, R. (2000). *Re-examine the two principles of special relativity and the Sagnac effect using GPS range measurement equation.* Position Location and Navigation Symposium, San Diego, CA, USA., 162-169.

21. Cernigliaro, A., Valloreia, S., Galleani, L., Travella, P. (2013). *GNSS space clocks: Performance analysis.* 2013 International Conference on Localization and GNSS (ICL-GNSS), Turin, Italy, 1-5.

22. Langley, R. B. (1999, May). Dilution of precision. *GPS World*, 10(5), 52-59.

23. Tahsin, M., Sultana, S., Reza, T., Hossam-E-Haider, M. (2015). *Analysis of DOP and its preciseness in GNSS position estimation.* 2015 International Conference on Electrical Engineering and Information Communication Technology (ICEEICT), Savar, Bangladesh, 1-6.

24. Tian, A., Dong, D., Ning, D., Fu, C. (2013). *GPS single point positioning algorithm based on least squares.* 2013 Sixth International Symposium on Computational Intelligence and Design, Hangzhou, China, 16-19.

25. Li, J., Muqing, W. (2009). *The improvement of positioning accuracy with weighted least square based on SNR.* 2009 5th International Conference on Wireless Communications, Networking and Mobile Computing, Bejing, China, 1-4.

26. Sedeek, A., Doma, M. (2014, January). Estimation of GPS receiver position using iterative least squares and extended Kalman filter. *Engineering Research Journal*, 37(1), 115-121.

27. Bancroft, S. (1985, January). An algebraic solution of the GPS equations. *IEEE Transactions on Aerospace and Electronic Systems*, AES-21(1), 56-59.

28. Ochieng, W., Sauer, K., Cross, P., Sheridan, K., Lannelongue, S., Ammour, N., Petit, K. (2002, December). Intergrity mechanisms for GPS satellites within the GALILEO architecture. *Journal of Geospatial Engineering*, 4(2), 95-110.

29. Raquet, J. (2013, May). *Calculation of GPS PNT solution.* Workshop on GNSS Data Application to Low Latitude Ionospheric Research, Trieste, Italy, 28-44.

30. Internet: Crustal Dynamics Data Information System (CDDIS DAAC), International GNSS Service (IGS). (2023). Daily 30-second observation data on January 31, 2023 from AMC400USA station. URL: https://cddis.nasa.gov/archive/gnss/data/daily/2023/004/23o/ Last Accessed on October 3, 2023.

31. Internet: Crustal Dynamics Data Information System (CDDIS DAAC), International GNSS Service (IGS). (2023). Daily navigation data on January 31, 2023 from AMC400USA station. URL: https://cddis.nasa.gov/archive/gnss/data/daily/2023/004/23n Last Accessed on September 3, 2023.

32. Internet: Mahooti, M. (2019, November 26). GPS receiver position. (v1.1.1.0). URL: https://www.mathworks.com/matlabcentral/fileexchange/56730-gps-receiver-position Last Accessed on September 7, 2023.

33. Simon, D. (2006). *Optimal state estimation: Kalman, H∞, and nonlinear approaches.* (1 ed.). New Jersey: John Wiley & Sons, 79-93.

34. Bedin, D. A. (2022). *Positioning by pseudorange measurements using the Bancroft method: Approaches to the description of the nonlinear error distribution.* 2022 29th Saint Petersburg International Conference on Integrated Navigation Systems (ICINS), Saint Petersburg, Russian Federation, 1-4.

35. Internet: International GNSS Service (IGS). (2023, February 15). RINEX. URL: https://igs.org/wg/rinex/#documents-formats Last Accessed on October 27, 2023.

36. Internet: Bislin, W. (2020, July 31). Understanding GPS/GNSS RINEX files and relevant parameters. URL: http://walter.bislins.ch/bloge/index.asp?page=Understanding+GPS%2FGNSS+RINEX+Files+and+Relevant+Parameters Last Accessed on October 27, 2023.

37. Internet: Aaron T. Becker's Robot Swarm Lab. (2023). Multilateration algebraic GPS equations (S. Bancroft method). (v1.0.3). URL: https://www.mathworks.com/matlabcentral/fileexchange/87744-multilateration-algebraic-gps-equations-s-bancroft-method Last Accessed on September 17, 2023.

38. Internet: Gürcan, N. (2023, November 28). Comparison GPS pseudorange algorithms. URL: https://github.com/nurullahgurcan/ComparisonGpsPseudorangeAlgorithms Last Accessed on November 28,2023.

39. Internet: Rebischung, P. (2023 (UTC), February 6). Possible co-seismic displacements: ANK2, ARUC, BSHM, BUCU, DRAG, HAMD, ISBA, ISTA, IZMI, KRS1, MERS, MIKL, NICO, RAMO, TUBI, ZECK. URL: https://lists.igs.org/pipermail/igsstation/2023/007687.html Last Accessed on October 27, 2023.

40. Schön, S., Bielenberg, O. (2008). *On the capability of high sensitivity GPS for precise indoor positioning.* 2008 5th Workshop on Positioning, Navigation and Communication, Hannover, Germany, 121-127.

APPENDICES

APPENDIX 1. Observation RINEX File

```
     2.11           OBSERVATION DATA    M (MIXED)           RINEX VERSION / TYPE
teqc  2018Dec12     gpsops              20230131 00:07:36UTCPGM / RUN BY / DATE
Linux 2.6.32-573.12.1.x86_64|x86_64|gcc -static|Linux 64|=+ COMMENT
BIT 2 OF LLI FLAGS DATA COLLECTED UNDER A/S CONDITION       COMMENT
AMC4                                                        MARKER NAME
40472S005                                                   MARKER NUMBER
GGN                 USNO                                    OBSERVER / AGENCY
3013929             SEPT POLARX5TR      5.4.0               REC # / TYPE / VERS
1364-10065          TPSCR.G5C       NONE                    ANT # / TYPE
 -1248596.2520 -4819428.2840  3976506.0340                  APPROX POSITION XYZ
        0.0000        0.0000        0.0000                  ANTENNA: DELTA H/E/N
     1     1                                                WAVELENGTH FACT L1/2
     7    L1    L2    P1    P2    C1    S1    S2           # / TYPES OF OBSERV
    30.0000                                                 INTERVAL
Forced Modulo Decimation to 30 seconds                      COMMENT
This data is provided as a public service by NASA/JPL.      COMMENT
No warranty is expressed or implied regarding suitability   COMMENT
for use.  For further information, contact:                 COMMENT
ggnops at jpl dot nasa dot gov                              COMMENT
 SNR is mapped to RINEX snr flag value [0-9]                COMMENT
  L1 & L2: min(max(int(snr_dBHz/6), 0), 9)                  COMMENT
  2023     1    30     0     0    0.0000000     GPS         TIME OF FIRST OBS
    18                                                      LEAP SECONDS
                                                            END OF HEADER
 23  1 30  0  0  0.0000000  0 32S31E19E13G06G30G24E15E21R12S33E27G19
                               R22E30G17E01R11G14S35G13G03G12E04G11
                               E26R10R13R23R21E20E14G01
 197218565.163 8                                                37529462.983
        49.500
 154697475.660 5                                                29437951.457
        34.500
 124020321.178 8                                                23600255.126
        49.250
 109369005.092 8  85222667.53748  20812205.631    20812206.958    20812205.684
        50.500          50.000
 130917532.706 6 102013681.89643  24912777.712    24912783.435    24912778.355
        36.500          23.500
 116785781.351 7  91001957.79946  22223573.655    22223575.470    22223573.851
        46.000          41.250
```

APPENDIX 2. Navigation RINEX File

```
     3.04           N: GNSS NAV DATA    G: GPS              RINEX VERSION / TYPE
sbf2rin-15.6.1                          20230131 000702 UTC PGM / RUN BY / DATE
GPSA   1.7695E-08 -7.4506E-09 -5.9605E-08  1.1921E-07       IONOSPHERIC CORR
GPSB   1.3107E+05 -1.3107E+05  6.5536E+04 -2.6214E+05       IONOSPHERIC CORR
GPUT  1.8626451492E-09 0.000000000E+00 319488 2247          TIME SYSTEM CORR
    18                                                      LEAP SECONDS
AMC4                                    MARKER NAME         COMMENT
40472S005                               MARKER NUMBER       COMMENT
 -1248596.2520 -4819428.2840  3976506.0340                  COMMENT
This data is provided as a public service by NASA/JPL.      COMMENT
No warranty is expressed or implied regarding suitability   COMMENT
for use.  For further information, contact:                 COMMENT
ggnops at jpl dot nasa dot gov                              COMMENT
                                                            END OF HEADER
G01 2023 01 30 00 00 00 2.185096964240E-04-4.433786671143E-12 0.000000000000E+00
     1.790000000000E+02-5.984375000000E+01 3.942664227791E-09 8.680611292018E-01
    -2.970919013023E-06 1.226864813361E-02 6.247311830521E-06 5.153655653000E+03
     8.640000000000E+04-1.024454832077E-07-1.885420718472E+00 1.136213541031E-07
     9.892025855611E-01 2.751250000000E+02 9.366878246705E-01-8.076765001110E-09
    -2.335811581642E-10 1.000000000000E+00 2.247000000000E+03 0.000000000000E+00
     2.000000000000E+00 6.300000000000E+01 4.656612873077E-09 1.790000000000E+02
     7.921800000000E+04 4.000000000000E+00
G03 2023 01 30 00 00 00-3.684819675982E-04 3.410605131648E-12 0.000000000000E+00
     4.900000000000E+01-4.640625000000E+01 4.086241636937E-09-2.789394894865E-01
    -2.456828951836E-06 4.455263726413E-03 8.661299943924E-06 5.153734003067E+03
     8.640000000000E+04-1.490116119385E-08-8.534378615240E-01 1.080334186554E-07
     9.773507576678E-01 2.208125000000E+02 1.021934049255E+00-7.867470568871E-09
     2.325096849617E-10 1.000000000000E+00 2.247000000000E+03 0.000000000000E+00
     2.000000000000E+00 0.000000000000E+00 1.862645149231E-09 4.900000000000E+01
     8.242800000000E+04 4.000000000000E+00
G06 2023 01 30 00 00 00 5.658175796270E-04 5.229594535194E-12 0.000000000000E+00
     7.000000000000E+01-7.350000000000E+01 3.869446892280E-09 1.126609326886E+00
    -3.894791007042E-06 2.896769554354E-03 5.546957254410E-06 5.153603141785E+03
     8.640000000000E+04 5.774199962616E-08-1.893724703772E+00-3.539025783539E-08
     9.884621427416E-01 2.846875000000E+02-8.610703323156E-01-7.894971714404E-09
    -1.717928701483E-10 1.000000000000E+00 2.247000000000E+03 0.000000000000E+00
     2.000000000000E+00 0.000000000000E+00 3.725290298462E-09 7.000000000000E+01
     7.980600000000E+04 4.000000000000E+00
```

Gazili olmak ayrıcalıktır